

APPENDIX C

DATA INTERPRETATION and CALCULATIONS

TABLE OF CONTENTS - APPENDIX C

C-1	INTRODUCTION	C1-5
C-2	PREPARATION OF GEOLOGIC BORING LOGS, HYDROGEOLOGIC SECTIONS, AND MAPS	C2-6
C.2.1	PREPARATION OF LITHOLOGIC LOGS	C2-6
C.2.2	PREPARATION OF HYDROGEOLOGIC SECTIONS	C2-7
C.2.3	REVIEW OF TOPOGRAPHIC MAPS AND PREPARATION OF POTENTIOMETRIC SURFACE MAPS AND FLOW NETS	C2-7
C.2.3.1	Review of Topographic Maps	C2-7
C.2.3.2	Preparation of Potentiometric Surface Maps	C2-7
C.2.3.3	Preparation of Flow Nets	C2-9
C.2.3.4	Preparation of Contaminant Isopach Maps	C2-9
C.2.3.5	Preparation of Contaminant and Daughter Product Isopleth Maps	C2-14
C.2.3.6	Preparation of Electron Donor, Inorganic Electron Acceptor, and Metabolic By-product Contour (Isopleth) Maps	C2-15
C-3	NATURAL ATTENUATION CALCULATIONS	C3-18
C.3.1	CALCULATING HYDRAULIC PARAMETERS	C3-18
C.3.1.1	Hydraulic Conductivity	C3-18
C.3.1.2	Transmissivity	C3-20
C.3.1.3	Hydraulic Head and Gradient	C3-20
C.3.1.4	Total Porosity (n) and Effective Porosity (n_e)	C3-23
C.3.1.5	Linear Ground-water Flow Velocity (Seepage or Advective Velocity)	C3-24
C.3.1.6	Coefficient of Retardation and Retarded Contaminant Transport Velocity	C3-25
C.3.2	CONTAMINANT SOURCE TERM CALCULATIONS	C3-28
C.3.2.1	Direct Measurement of Dissolved Contaminant Concentrations in Ground Water in Contact with NAPL	C3-31
C.3.2.2	Equilibrium Partitioning Calculations	C3-32
C.3.2.3	Mass Flux Calculations	C3-33
C.3.3	CONFIRMING AND QUANTIFYING BIODEGRADATION	C3-37
C.3.3.1	Isopleth Maps	C3-37
C.3.3.2	Data Set Normalization	C3-37
C.3.3.3	Calculating Biodegradation Rates	C3-41
C.3.4	DESIGN, IMPLEMENTATION, AND INTERPRETATION OF MICROCOSM STUDIES	C3-49
C.3.4.1	Overview	C3-49
C.3.4.2	When to Use Microcosms	C3-50
C.3.4.3	Application of Microcosms	C3-50
C.3.4.4	Selecting Material for Study	C3-50
C.3.4.5	Geochemical Characterization of the Site	C3-51
C.3.4.6	Microcosm Construction	C3-54
C.3.4.7	Microcosm Interpretation	C3-54
C.3.4.8	The Tibbetts Road Case Study	C3-55
C.3.4.9	Summary	C3-58

FIGURES

No.	Title	Page
C.2.1	Example hydrogeologic section	C2-6
C.2.2	Example ground-water elevation map	C2-8
C.2.3	Example flow net	C2-9
C.2.4	Example mobile LNAPL isopach (A) and contaminant isopleth (B) maps	C2-10
C.2.5	Measured (apparent) <i>versus</i> actual LNAPL thickness	C2-11
C.2.6	Type curve for LNAPL baildown test	C2-14
C.2.7	Example isopleth maps of contaminants and soluble electron acceptors	C2-16
C.2.8	Example isopleth maps of contaminants and metabolic by-products	C2-17
C.3.1	Range of hydraulic conductivity values	C3-18
C.3.2	Hydraulic head	C3-21
C.3.3	Ground-water Elevation Map	C3-23
C.3.4	Location of sampling points at the St. Joseph, Michigan NPL site	C3-25
C.3.5	Field rate constants for TCE as reported in literature	C3-43
C.3.6	Field rate constants for PCE as reported in literature	C3-43
C.3.7	Field rate constants for Vinyl Chloride as reported in literature	C3-44
C.3.8	Exponential regression of TCE concentration on time of travel along flow path	C3-46
C.3.9	Regression of the TCE concentration on distance along flow path	C3-48
C.3.10	Tibbetts Road study site	C3-49
C.3.11	TCE microcosm results	C3-56
C.3.12	Benzene microcosm results	C3-56
C.3.13	Toluene microcosm results	C3-57

TABLES

No.	Title	Page
C.2.1	Typical Values for $h_{aw}^c _{dr}$	C2-12
C.2.2	Surface Tensions for Various Compounds	C2-13
C.2.3	Results of Example Baildown Test	C2-15
C.3.1	Representative Values of Hydraulic Conductivity for Various Sediments and Rocks	C3-19
C.3.2	Representative Values of Dry Bulk Density, Total Porosity, and Effective Porosity for Common Aquifer Matrix Materials	C3-24
C.3.3	Representative Values of Total Organic Carbon for Common Sediments	C3-27
C.3.4	Example Retardation Calculations for Select Compounds	C3-28
C.3.5	Attenuation of Chlorinated Ethenes and Chloride Downgradient of the Source of TCE in the West Plume at the St. Joseph, Michigan, NPL Site	C3-40
C.3.6	Use of the Attenuation of a Tracer to Correct the Concentration of TCE Downgradient of the Source of TCE in the West Plume at the St. Joseph, Michigan NPL Site	C3-41
C.3.7	Geochemical Parameters Important to Microcosm Studies	C3-53
C.3.8	Contaminants and Daughter Products	C3-53
C.3.9	Concentrations of TCE, Benzene, and Toluene in the Tibbetts Road Microcosms	C3-58
C.3.10	First-order Rate Constants for Removal of TCE, Benzene, and Toluene in the Tibbetts Road Microcosms	C3-59
C.3.11	Concentrations of Contaminants and Metabolic By-products in Monitoring Wells along Segments in the Plume used to Estimate Field-scale Rate Constants	C3-59
C.3.12	Comparison of First-order Rate for Contaminant Attenuation in Segments of the Tibbetts Road Plume	C3-60
C.3.13	Comparison of First-order Rate Constants in a Microcosm Study, and in the Field at the Tibbetts Road NPL Site	C3-60

SECTION C-1

INTRODUCTION

Successful documentation of natural attenuation requires interpretation of site-specific data to define the ground-water flow system, refine the conceptual model, quantify rates of contaminant attenuation, and model the fate and transport of dissolved contaminants. Tasks to be completed include preparation of lithologic logs, hydrogeologic sections, potentiometric surface maps and flow nets, contaminant isopach and isopleth maps, electron acceptor and metabolic byproduct isopleth maps, and calculation of hydraulic parameters, retardation coefficients, and biodegradation rate constants. The rate and amount of partitioning of organic compounds from mobile and residual nonaqueous-phase liquid (NAPL) into ground water should also be determined to allow estimation of a source term. Completion of these tasks permits refinement of the conceptual model and is necessary to successfully support remediation by natural attenuation.

This appendix consists of three sections, including this introduction. Section C-2 discusses preparation of geologic boring logs, hydrogeologic sections, and maps. Section C-3 covers natural attenuation calculations, including hydraulic parameter calculations, contaminant source term calculations, confirming and quantifying biodegradation, and designing, implementing, and interpreting microcosm studies.

SECTION C-2

PREPARATION OF GEOLOGIC BORING LOGS, HYDROGEOLOGIC SECTIONS, AND MAPS

The first step after completion of site characterization field activities is to prepare geologic boring logs, hydrogeologic sections, water table elevation (or potentiometric surface) maps, flow nets, and maps depicting contaminant concentrations, electron acceptor and metabolic byproduct concentrations, and mobile NAPL thickness. The construction of these items is discussed in the following sections.

C.2.1 PREPARATION OF LITHOLOGIC LOGS

Lithologic logs should be prepared using field data. Whenever possible, these logs should contain descriptions of the aquifer matrix, including relative density, color, major textural constituents, minor constituents, porosity, relative moisture content, plasticity of fines, cohesiveness, grain size, structure or stratification, relative permeability, and any significant observations such as visible fuel or fuel odor. It is also important to correlate the results of volatile organic compound (VOC) screening using headspace vapor analysis with depth intervals of geologic materials. The depth of lithologic contacts and/or significant textural changes should be recorded to the nearest 0.1 foot. This resolution is necessary because preferential flow and contaminant transport pathways may be limited to stratigraphic units less than 6 inches thick.

C.2.2 PREPARATION OF HYDROGEOLOGIC SECTIONS

Lithologic logs should be used in conjunction with water level data to prepare a minimum of two hydrogeologic sections for the site. One section should be oriented parallel to the direction of ground-water flow, and one section should be oriented perpendicular to the direction of ground-water flow. Both sections should be drawn to scale. Hydrogeologic sections are an integral part of the conceptual model and are useful in identifying preferential contaminant migration pathways and in modeling the site.

At a minimum, hydrogeologic sections should contain information on the relationships between hydrostratigraphic units at the site, including the location and distribution of transmissive vs. non-transmissive units, the location of the water table relative to these units, and the location(s) of the contaminant source(s). Figure C.2.1 is an example of a completed hydrogeologic section.

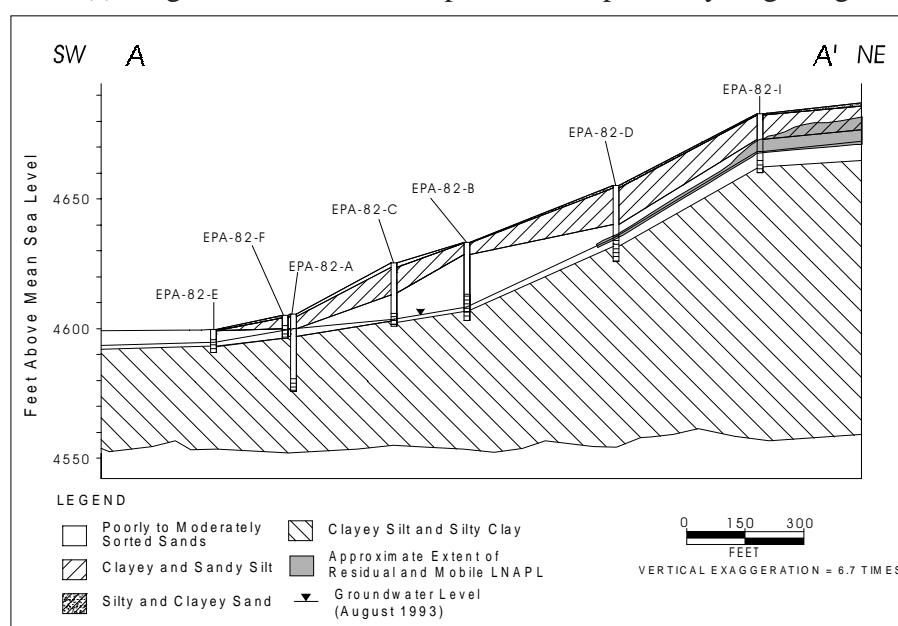


Figure C.2.1 Example hydrogeologic section.

C.2.3 REVIEW OF TOPOGRAPHIC MAPS AND PREPARATION OF POTENTIOMETRIC SURFACE MAPS AND FLOW NETS

Determining the direction of ground-water flow and the magnitude of hydraulic gradients is important because these parameters influence the direction and rate of contaminant migration. Ground-water flow directions are represented by a three-dimensional set of equipotential lines and orthogonal flow lines. If a plan view (potentiometric surface, or water table elevation, map) or a two-dimensional cross-section is drawn to represent a flow system, the resultant equipotential lines and flow lines constitute a flow net. A flow net can be used to determine the distribution of hydraulic head, the ground-water velocity distribution, ground-water and solute flow paths and flow rates, and the general flow pattern in a ground-water system.

C.2.3.1 Review of Topographic Maps

Ground-water flow is strongly influenced by the locations of ground-water divides and by recharge from and discharge to surface water bodies such as rivers, streams, lakes, and wetlands. Topographic highs generally represent divergent flow boundaries (divergent ground-water divide), and topographic lows such as valleys or drainage basins typically represent convergent flow boundaries (convergent ground-water divide). In addition, the configuration of the water table is typically a subtle reflection of the surface topography in the area. However, topography is not always indicative of subsurface flow patterns and should not be depended upon unless confirmed by head data. In order to place the local hydrogeologic flow system within the context of the regional hydrogeologic flow system, it is important to have an understanding of the local and regional topography. Included in this must be knowledge of the locations of natural and manmade surface water bodies. This information can generally be gained from topographic maps published by the United States Geological Survey.

C.2.3.2 Preparation of Potentiometric Surface Maps

A potentiometric surface map is a two-dimensional graphical representation of equipotential lines shown in plan view. Water table elevation maps are potentiometric surface maps drawn for water table (unconfined) aquifers. Potentiometric surface maps for water table aquifers show where planes of equal potential intersect the water table. A potentiometric surface map should be prepared from water level measurements and surveyor's data. These maps are used to estimate the direction of plume migration and to calculate hydraulic gradients. To document seasonal variations in ground-water flow, separate potentiometric surface maps should be prepared using quarterly water level measurements taken over a period of at least 1 year.

The data used to develop the potentiometric surface map should be water level elevation data (elevation relative to mean sea level) from piezometers/wells screened in the same relative position within the same hydrogeologic unit. For example, wells that are screened at the water table can be used for the same potentiometric surface map. Wells screened in different hydrogeologic units or at different relative positions within the same water table aquifer cannot be used to prepare a potentiometric surface map. Where possible, a potentiometric surface map should be prepared for each hydrogeologic unit at the site. In recharge areas, wells screened at various elevations cannot all be used to prepare the same potentiometric surface map because of strong downward vertical gradients. Likewise, wells screened at various elevations in discharge areas such as near streams, lakes, or springs, should not all be used because of the strong upward vertical gradients.

When preparing a potentiometric surface map, the locations of system boundaries should be kept in mind; particularly the site features that tend to offset the shape of the contours on the map. Such features include topographic divides, surface water bodies, and pumping wells.

In addition to, and separately from, preparation of a potentiometric surface map, water level measurements from wells screened at different depths can be used to determine any vertical hydroau-

lic gradients. It is important to have a good understanding of vertical hydraulic gradients because they may have a profound influence on contaminant migration.

In areas with measurable mobile LNAPL, a correction must be made for the water table deflection caused by the LNAPL. The following relationship, based on Archimedes' Principle, provides a correction factor that allows the water table elevation to be adjusted for the effect of floating LNAPL.

$$CDTW = MDTW - \frac{\rho_{lnapl}}{\rho_w} (PT) \quad \text{eq. C.2.1}$$

Where:

$CDTW$ = corrected depth to water [L]

$MDTW$ = measured depth to water [L]

ρ_{lnapl} = density of the LNAPL [M/L³]

ρ_w = density of the water, generally 1.0 [M/L³]

PT = measured LNAPL thickness [L]

Using the corrected depth to water, the corrected ground-water elevation, CGWE, is given by:

$$CGWE = \text{Datum Elevation} - CDTW \quad \text{eq. C.2.2}$$

Corrected ground-water elevations should be used for potentiometric surface map preparation.

Figure C.2.2 is an example of a ground-water elevation map for an unconfined aquifer. Water table elevation data used to prepare this map were taken from wells screened across the water table.

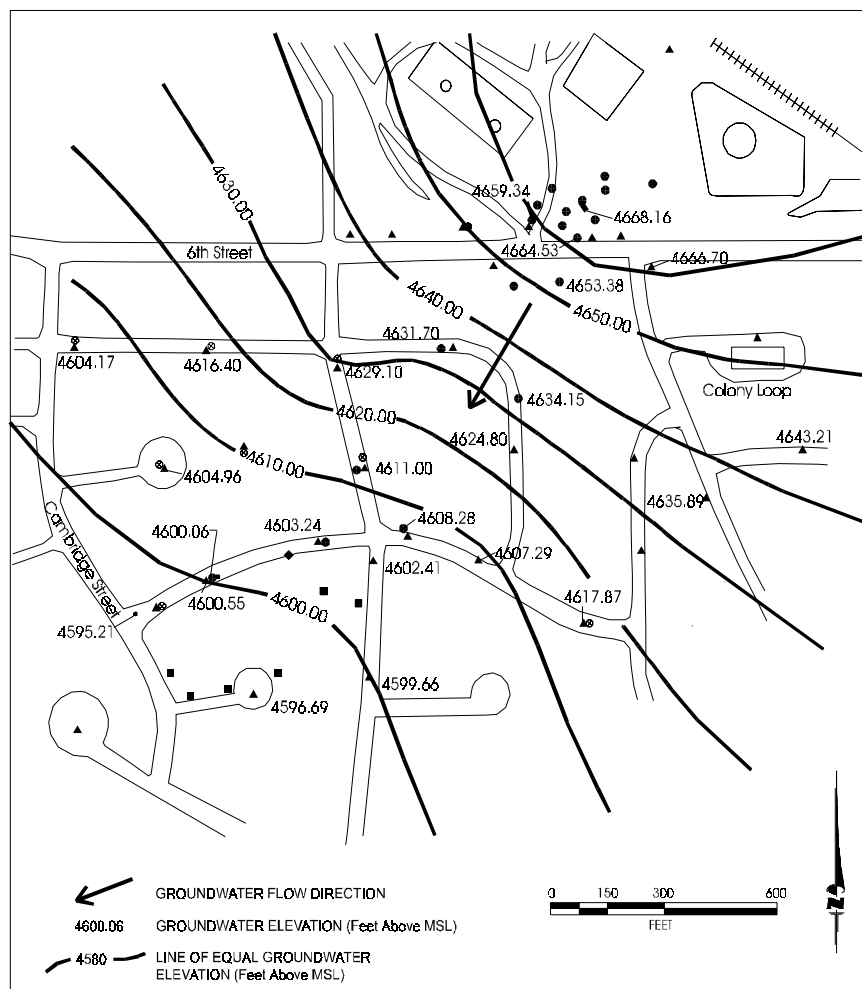


Figure C.2.2 Example ground-water elevation map.

C.2.3.3 Preparation of Flow Nets

Where an adequate three-dimensional database is available, flow nets can be constructed to facilitate the interpretation of the total hydraulic head distribution in the aquifer. This will help determine potential solute migration pathways. The simplest ground-water flow system is one that is homogeneous and isotropic. This type of hydrogeologic setting serves as a simple basis for describing the basic rules of flow net construction, despite the fact that homogeneous, isotropic media rarely occur in nature. Regardless of the type of geologic media, the basic rules of flow net construction must be applied, and necessary modifications must be made throughout the procedure to account for aquifer heterogeneity or anisotropic conditions. Water level data for flow net construction should come from multiple sets of nested wells (two or more wells at the same location) at various depths in the aquifer. The fundamental rules of flow net construction and the important properties of flow nets are summarized as follows:

- Flow lines and equipotential lines intersect at 90-degree angles if the permeability is isotropic;
- The geometric figures formed by the intersection of flow lines and equipotential lines must approximate squares or rectangles;
- Equipotential lines must meet impermeable boundaries at right angles (impermeable boundaries are flow lines); and
- Equipotential lines must be parallel to constant-head boundaries (constant-head boundaries are equipotential lines).

Trial-and-error sketching is generally used to construct a flow net. Flow net sketching can be sufficiently accurate if constructed according to the basic rules outlined above. A relatively small number of flow lines (three to five) generally are sufficient to adequately characterize flow conditions. Flow nets should be superimposed on the hydrogeologic sections. Figure C.2.3 is an example of a completed flow net. This figure shows ground-water flow patterns in both recharge and discharge areas.

C.2.3.4 Preparation of Contaminant Isopach Maps

If NAPL is present at the site, isopach maps showing the thickness and distribution of NAPL should be prepared. Two maps should be prepared: one for mobile NAPL, and one for residual NAPL. Such isopach maps allow estimation of the distribution of NAPL in the subsurface and aid in

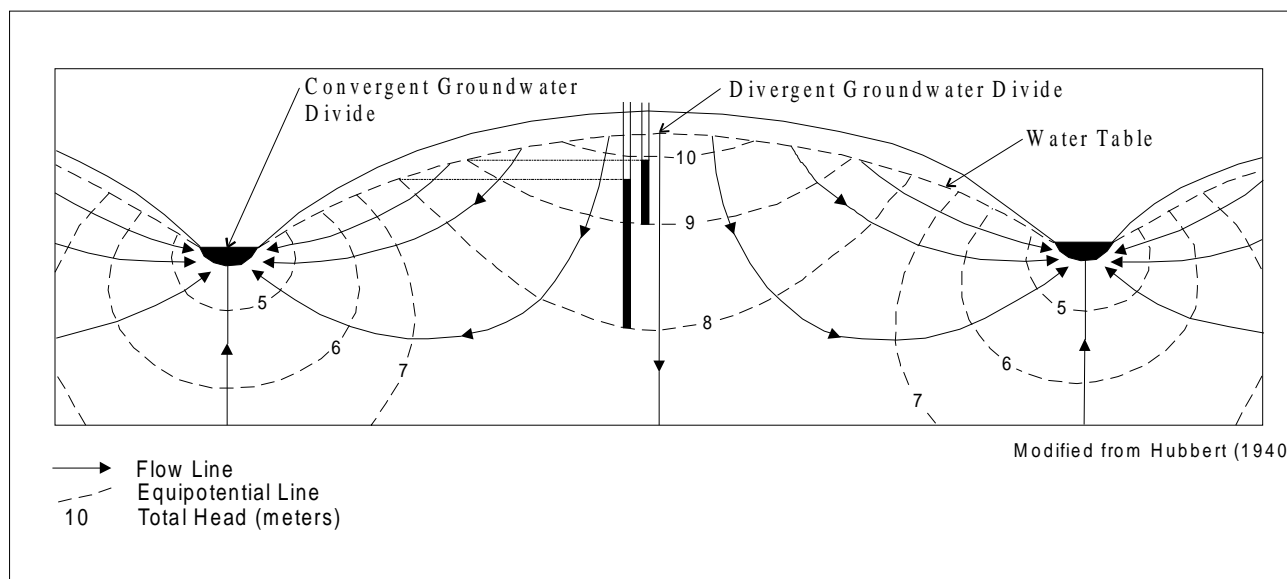


Figure C.2.3 Example flow net.

fate and transport model development by identifying the boundary of the NAPL. Because of the differences between the magnitude of capillary suction in the aquifer matrix and the different surface tension properties of fuel and water, LNAPL thickness observations made in monitoring points are only an estimate of the actual volume of mobile LNAPL in the aquifer. To determine the actual NAPL thickness it is necessary to collect and visually analyze soil samples. LNAPL thickness data also should be used to correct for water table deflections caused by the mobile LNAPL. This process is described in Section C.2.2.3.2.

Isopach maps are prepared by first plotting the measured NAPL thickness on a base map prepared using surveyor's data. Lines of equal NAPL thickness (isopachs) are then drawn and labeled. Each data point must be honored during contouring. Figure C.2.4 is an example of a completed isopach map. This figure also contains an example of an isopleth map.

C.2.3.4.1 Relationship Between Apparent and Actual LNAPL Thickness

It is well documented that LNAPL thickness measurements taken in ground-water monitoring wells are not indicative of actual LNAPL thicknesses in the formation (de Pastovich *et al.*, 1979; Blake and Hall, 1984; Hall *et al.*, 1984; Hughes *et al.*, 1988; Abdul *et al.*, 1989; Testa and Paczkowski, 1989; Farr *et al.*, 1990; Kemblowski and Chiang, 1990; Lenhard and Parker, 1990; Mercer and Cohen, 1990; Ballesterio *et al.*, 1994; Huntley *et al.*, 1994a). These authors note that the measured thickness of LNAPL in a monitoring well is greater than the true LNAPL thickness in the aquifer and, according to Mercer and Cohen (1990), measured LNAPL thickness in wells is typically 2 to 10 times greater than the actual LNAPL thickness in the formation. The difference between actual and measured LNAPL thickness occurs because mobile LNAPL floating on the water table flows into the well (if the top of well screen is above the base of the LNAPL) and depresses the water table. Figure C.2.5 is a schematic that illustrates this relationship. The equation for correcting depth

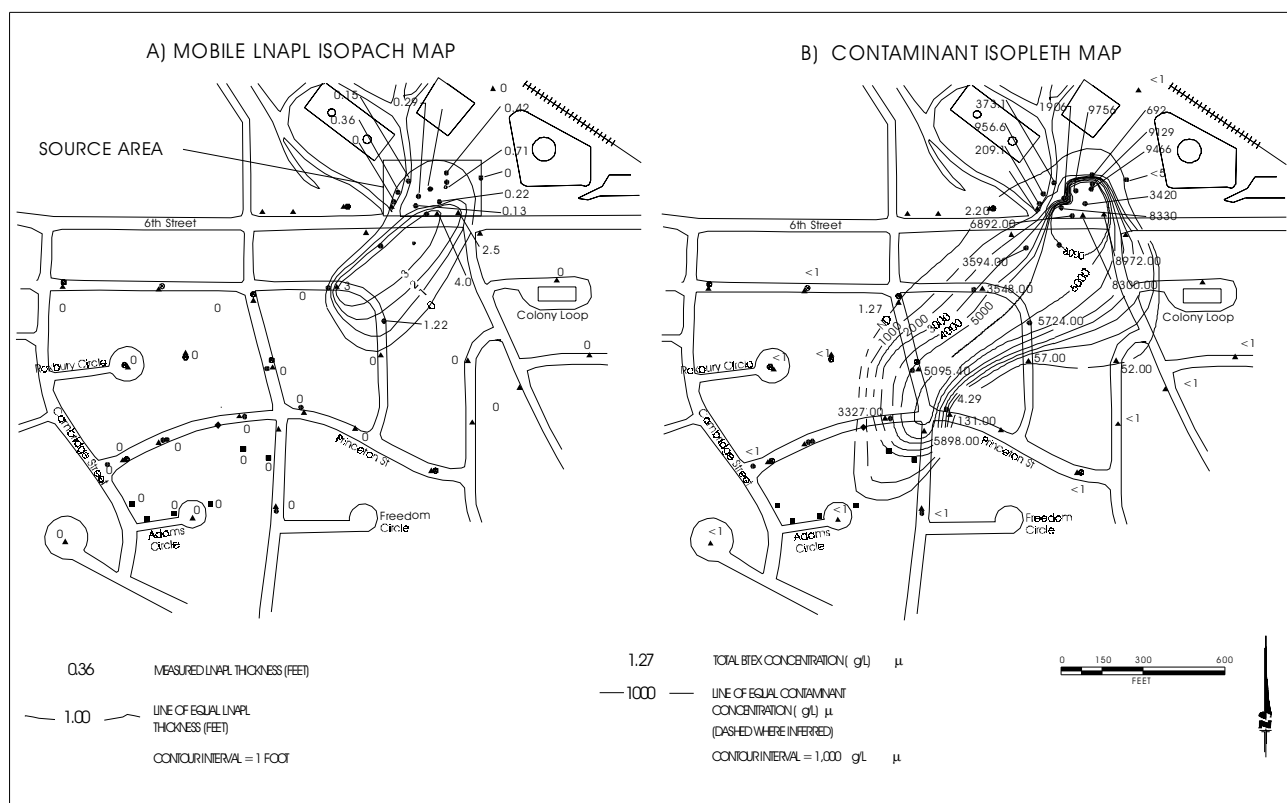


Figure C.2.4 Example mobile LNAPL isopach (A) and contaminant isopleth (B) maps.

to ground water caused by LNAPL in the well is given in Section C.2.3.2. Empirical relationships relating measured LNAPL thickness to actual LNAPL thickness are presented below. Also presented below are test methods that can be used to determine actual LNAPL thickness. There are no established methods for determining actual DNAPL volume based on measurements taken in monitoring wells.

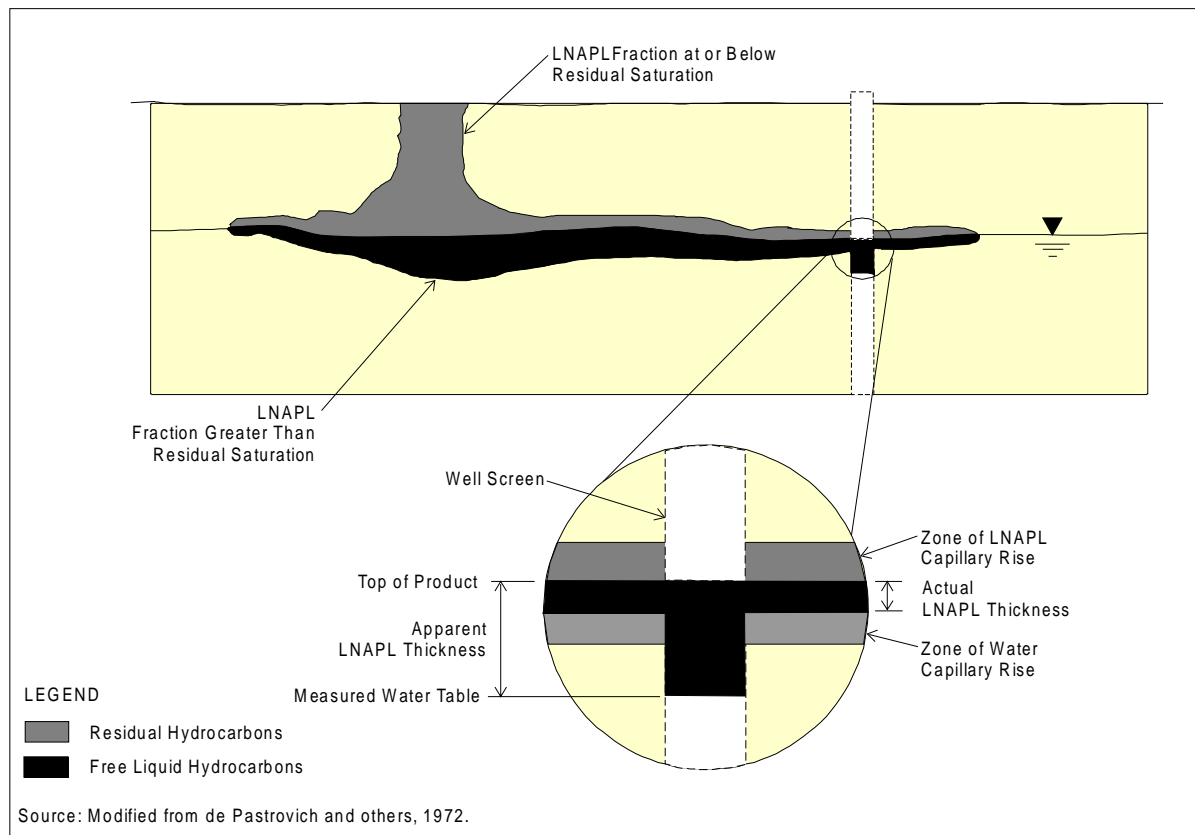


Figure C.2.5 Measured (apparent) versus actual LNAPL thickness.

C.2.3.4.2. Empirical Relationships

There are several empirical methods available to estimate the actual thickness of mobile LNAPL in the subsurface based on LNAPL thicknesses measured in a ground-water monitoring well. Such empirical relationships are, at best, approximations because many factors influence the relationship between measured and apparent LNAPL thickness (Mercer and Cohen, 1990):

- Capillary fringe height depends on grain size and is hysteretic with fluid level fluctuations.
- LNAPL can become trapped below the water table as the water table rises and falls.
- The thickness of LNAPL is ambiguous because the interval of soil containing mobile LNAPL is not 100-percent saturated with LNAPL.

Some empirical methods for determining actual LNAPL thickness are described below.

Method of de Pastrovich *et al.* (1979)

Hampton and Miller (1988) conducted laboratory experiments to examine the relationship between the actual thickness of LNAPL in a formation, h_p , and that measured in a monitoring well, h_m . Based on their research, Hampton and Miller (1988) suggest using the following relationship (developed by de Pastrovich *et al.*, 1979) to estimate LNAPL thickness:

$$h_f \approx \frac{h_m(\rho_w - \rho_{lnapl})}{\rho_{lnapl}} \quad \text{eq. C.2.3}$$

Where:

- h_f = actual thickness of LNAPL in formation
- h_m = measured LNAPL thickness in well
- ρ_w = density of water (1.0 gm/cm³ for pure water)
- ρ_{lnapl} = density of LNAPL (See Table C.3.9)

Method of Kemblowski and Chiang (1990)

Another empirical relationship was proposed by Kemblowski and Chiang (1990) to estimate actual LNAPL thickness based on measured LNAPL thickness. This relationship is given by:

$$h_o = H_o - 2.2h_{aw}^c|_{dr} \quad \text{eq. C.2.4}$$

Where:

- h_o = equivalent thickness of LNAPL in the formation (volume of oil per unit area of aquifer, divided by porosity)
- H_o = measured LNAPL thickness in well
- $h_{aw}^c|_{dr}$ = capillary height of air-water interface assuming water is being displaced by oil (typical values are given in Table C.2.1)

This method assumes equilibrium conditions, water drainage, and oil imbibition.

Table C.2.1 Typical Values for $h_{aw}^c|_{dr}$ (Bear, 1972)

Aquifer Matrix	$h_{aw}^c _{dr}$ (cm)	$h_{aw}^c _{dr}$ (ft)
Coarse Sand	2-5	0.066-0.16
Sand	12-35	0.39-1.15
Fine Sand	35-70	1.14-2.30
Silt	70-150	2.30-4.92
Clay	>200-400	>6.56-13.12

Method of Lenhard and Parker (1990)

Another empirical relationship was proposed by Lenhard and Parker (1990) to estimate actual LNAPL thickness based on measured LNAPL thickness. This relationship is given by:

$$D_o = \frac{\rho_{ro}\beta_{ao}H_o}{\beta_{ao}\rho_{ro} - \beta_{ow}(1 - \rho_{ro})} \quad \text{eq. C.2.5}$$

Where:

- D_o = actual thickness of LNAPL in formation
- H_o = measured LNAPL thickness in well
- ρ_{ro} = specific gravity of LNAPL (density of oil/density of water)
- $\beta_{ao} = \frac{\sigma_{aw}}{\sigma_{ao}}$ Air-oil scaling factor

$$\beta_{ow} = \frac{\sigma_{aw}}{\sigma_{ow}} \text{ Oil-water scaling factor}$$

σ_{aw} = surface tension of uncontaminated water (72.75 dynes/cm @ 20°C)

σ_{ao} = surface tension of LNAPL [25 dynes/cm @ 20°C for JP-4, Table C.2.2]

$\sigma_{ow} = \sigma_{aw} - \sigma_{ao}$ = interfacial tension between water and LNAPL (47.75 dynes/cm @ 20°C)

It is important to note that this method includes the capillary thickness of the hydrocarbon, and is, therefore, likely to be an overestimate.

Table C.2.2 Surface Tensions for Various Compounds

Compound	Surface Tension @ 20°C (dyne/cm)
JP-4	25 ^{a/}
Gasoline	19-23 ^{a/}
Pure Water	72.75 ^{b/}

a/ Martel (1987).

b/ CRC Handbook (1956).

C.2.3.4.3. LNAPL Baildown Test

The LNAPL baildown test is applicable in areas where the hydrocarbon/water interface is below the potentiometric surface, and the recharge rate of hydrocarbon into the well is slow (Hughes *et al.*, 1988).

Baildown Test Procedure (from Hughes *et al.*, 1988):

- 1) Gauge the well and calculate the corrected potentiometric surface elevation using equations C.2.1 and C.2.2.
- 2) Rapidly bail the hydrocarbon from the well.
- 3) Gauge the well again, and if the thickness of the hydrocarbon is acceptable (0.1 to 1 foot), calculate the potentiometric surface elevation. The potentiometric surface elevation thus calculated should be within 0.005 foot of the value calculated in step 1. If it is, then continue to step 4; if it is not, repeat steps 2 and 3.
- 4) Record the top of the LNAPL surface in the well as it recharges until the well is fully recharged.
- 5) Plot the elevation of the top of LNAPL in the well vs. time since bailing ceased.
- 6) The true thickness of the mobile LNAPL layer (T_f) is the distance from the inflection point to the top of the hydrocarbon under static conditions (Figure C.2.6). Thus, T_f is picked directly off the plot. Table C.2.3 is an example of the results of this procedure.

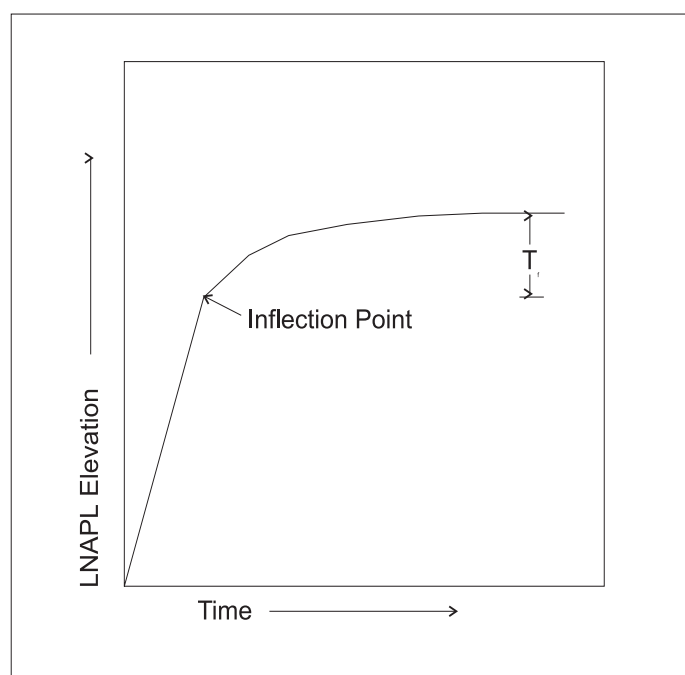


Figure C.2.6 Type curve for LNAPL baildown test.

Table C.2.3 Results of Example Baildown Test (Modified from Hughes *et al.*, 1988)

Well	T_w (ft) ^{a/}	T_f (ft)	Exaggeration (T_w/T_f)
ROW-143	4.97	0.61	8.1:1
ROW-189	12.5	0.29	43.0:1
ROW-129	0.94	0.0 ^{b/}	N/A

a/ T_w = LNAPL thickness initially measured in the well, if LNAPL thickness that is actually mobile

b/ Capillary oil only

Hughes *et al.* (1988) also present a recharge method that involves pumping the mobile LNAPL until steady-state conditions are achieved, and then letting the well fully recharge.

C.2.3.5 Preparation of Contaminant and Daughter Product Isopleth Maps

Isopleth maps should be prepared for all chlorinated solvents of concern and their daughter products and for total BTEX if present. For example, if trichloroethene and BTEX were released (as is typical for fire training areas), then maps of dissolved trichloroethene, dichloroethene, vinyl chloride, ethene, and total BTEX concentrations should be prepared. Isopleth maps allow interpretation of data on the distribution and the relative transport and degradation rates of contaminants in the subsurface. In addition, contaminant isopleth maps allow contaminant concentrations to be gridded and used for input into a solute transport model.

Isopleth maps are prepared by first plotting the concentration of the contaminant on a base map prepared using surveyor's data. Lines of equal contaminant concentration (isopleths) are then drawn

and labeled. It is important to ensure that each data point is honored during contouring. Outliers should be displayed and qualified, if they are not contoured. Figures C.2.4, C.2.7, and C.2.8 contain examples of contaminant isopleth maps.

Dissolved contaminant concentrations are determined through ground-water sampling and laboratory analysis. From these data, isopleth maps for each of the contaminant compounds and for total dissolved contaminant should be made. Dissolved BTEX concentrations are transferred to the fate and transport model grid cells by overlaying the isopleth map onto the model grid.

C.2.3.6 Preparation of Electron Donor, Inorganic Electron Acceptor, and Metabolic By-product Contour (Isopleth) Maps

Isopleth maps should be prepared for any organic compound that can be used as an electron donor. Examples of such compounds include natural organic carbon, and petroleum hydrocarbons (and landfill leachate). These maps are used to provide visible evidence that biodegradation could occur or is occurring. Isopleth maps also should be prepared for dissolved oxygen, nitrate, manganese (II), iron (II), sulfate, methane, and chloride. These maps are used to provide visible evidence that biodegradation is occurring. The electron acceptor and metabolic by-product isopleth maps can be used to determine the relative importance of each of the terminal electron-accepting processes (TEAPs).

Isopleth maps are prepared by first plotting the concentration of the electron donor, electron acceptor, or metabolic by-product on a base map prepared using surveyor's data. Lines of equal concentration (isopleths) are then drawn and labeled. It is important to ensure that each data point is honored during contouring, unless some data are suspect.

C.2.3.6.1 Inorganic Electron Acceptor Isopleth Maps

Electron acceptor isopleth maps allow interpretation of data on the distribution of dissolved oxygen, nitrate, and sulfate in the subsurface. Isopleth maps for these compounds provide a visual indication of the relationship between the contaminant plume and the electron acceptors and the

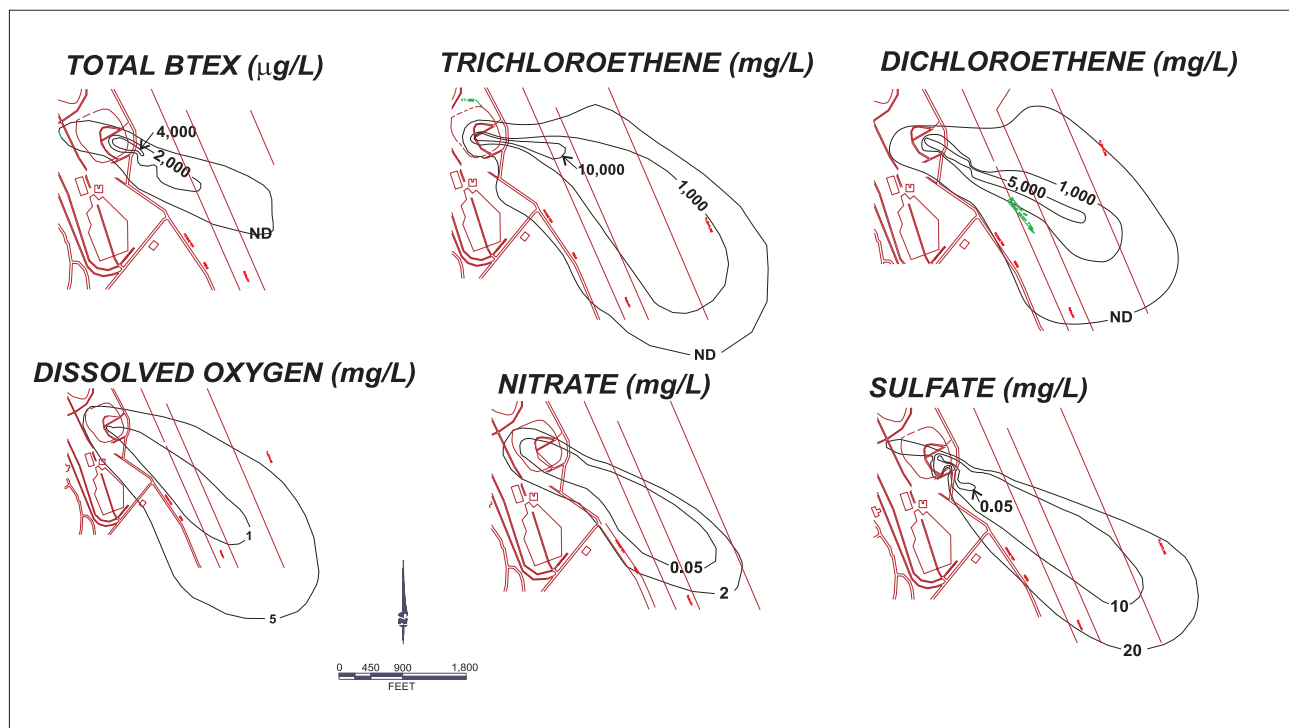


Figure C.2.7 Example isopleth maps of contaminants and soluble electron acceptors.

relative importance of each TEAP. Dissolved oxygen concentrations below background levels in areas with high organic carbon concentrations are indicative of aerobic respiration. Nitrate concentrations below background in areas with high organic carbon concentrations are indicative of denitrification. Sulfate concentrations below background in areas with high organic carbon concentrations are indicative of sulfate reduction.

Figure C.2.7 gives examples of completed isopleth maps for dissolved oxygen, nitrate, and sulfate. This figure also contains isopleth maps for TCE and DCE and the total BTEX (electron donor) isopleth map for the same period. Comparison of the total BTEX isopleth map and the electron acceptor isopleth maps shows that there is a strong correlation between areas with elevated organic carbon and depleted electron acceptor concentrations. The strong correlation indicates that the electron acceptor demand exerted during the metabolism of BTEX has resulted in the depletion of soluble inorganic electron acceptors. These relationships provide strong evidence that biodegradation is occurring via the processes of aerobic respiration, denitrification, and sulfate reduction.

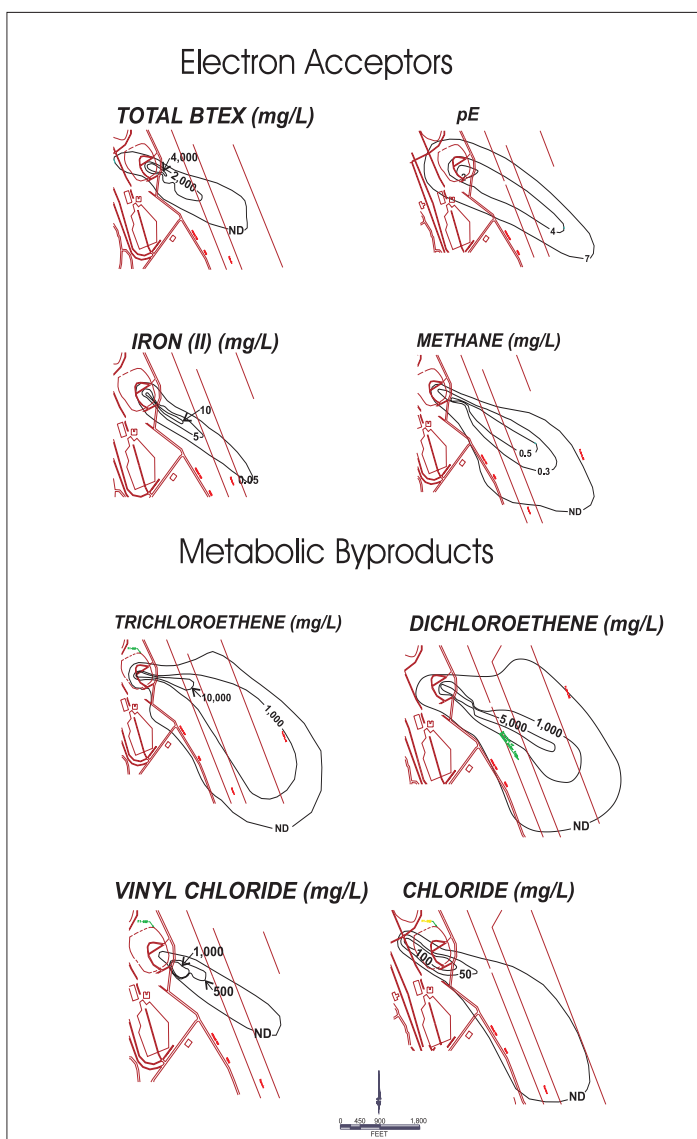


Figure C.2.8 Example isopleth maps of contaminants and metabolic by-products.

C.2.3.6.2 Metabolic By-product Isopleth Maps

Metabolic by-product maps should be prepared for manganese (II), iron (II), methane, and chloride. The manganese (II) map is prepared in lieu of an electron acceptor isopleth map for manganese (IV) because the amount of bioavailable amorphous or poorly crystalline manganese (IV) in an aquifer matrix is extremely hard to quantify. The iron (II) map is prepared in lieu of an electron acceptor isopleth map for iron (III) because the amount of bioavailable amorphous or poorly crystalline iron (III) in an aquifer matrix is extremely hard to quantify. Iron (II) concentrations above background levels in areas with BTEX contamination are indicative of anaerobic iron (III) reduction. Methane concentrations above background levels in areas with BTEX contamination are indicative of methanogenesis, another anaerobic process. Biodegradation of chlorinated solvents tends to increase the chloride concentration found in ground water. Thus, chloride concentrations inside the contaminant plume generally increase to concentrations above background. This map will allow visual interpretation of chloride data by showing the relationship between the contaminant plume and chloride. During anaerobic biodegradation, the oxidation-reduction potential of ground water is lowered. Thus, the oxidation-reduction potential (or pE) inside the contaminant plume generally decreases to levels below background.

Figure C.2.8 gives examples of completed isopleth maps for iron (II), methane, chloride, and pE. This figure also contains the TCE, DCE and Vinyl Chloride isopleth maps, and total BTEX (electron donor) isopleth map for the same period. Comparison of the total BTEX isopleth map and the metabolic by-product isopleth maps and comparison of Figures C.2.7 and C.2.8 shows that there is a strong correlation between areas with elevated organic carbon and elevated metabolic by-product concentrations. These relationships provide strong evidence that biodegradation is occurring via the processes of iron (III) reduction, methanogenesis, and reductive dechlorination.

SECTION C-3

NATURAL ATTENUATION CALCULATIONS

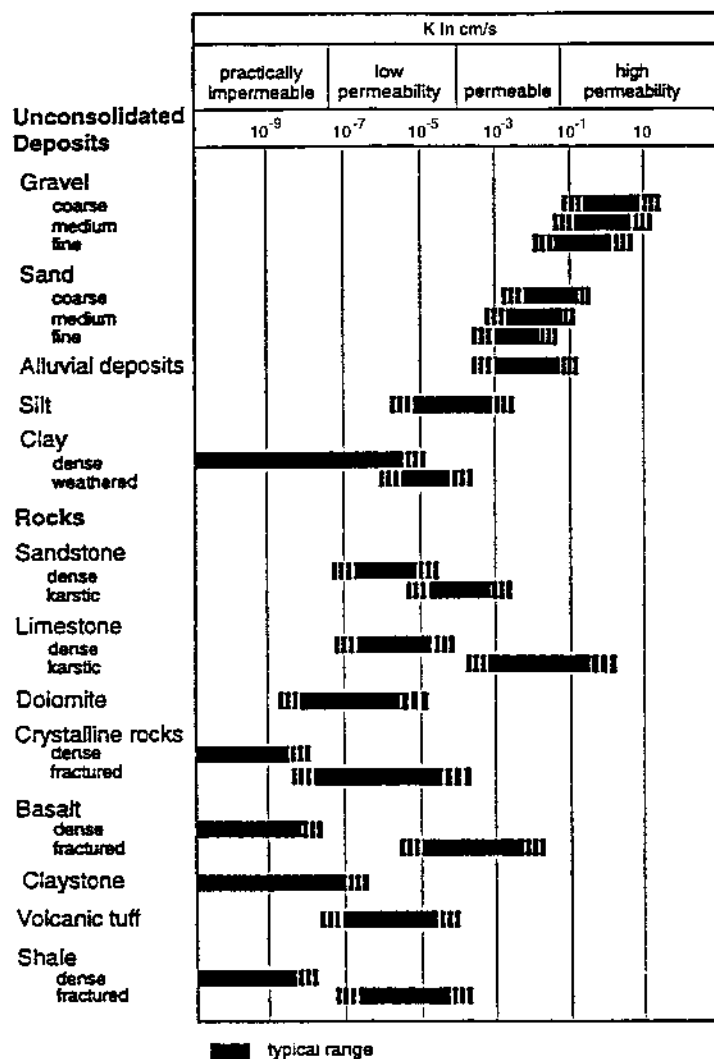
Several calculations using site-specific data must be made in order to document the occurrence of natural attenuation and successfully implement the natural attenuation alternative. The following sections describe these calculations.

C.3.1 CALCULATING HYDRAULIC PARAMETERS

Hydraulic parameters necessary for adequate site characterization and model implementation include hydraulic conductivity, transmissivity, hydraulic gradient, linear ground-water flow velocity, hydrodynamic dispersion, and retarded solute transport velocity. Calculations for these parameters are discussed in the following sections.

C.3.1.1 Hydraulic Conductivity

Hydraulic conductivity, K , is a measure of an aquifer's ability to transmit water and is perhaps the most important variable governing fluid flow in the subsurface. Hydraulic conductivity has the units of length over time [L/T]. Observed values of hydraulic conductivity range over 12 orders of magnitude, from 3×10^{-12} to 3 cm/sec (3×10^{-9} to 3×10^3 m/day) (Figure C.3.1 and Table C.3.1). In



Modified from: Spitz and Moreno, 1996.

Figure C.3.1 Range of hydraulic conductivity values.

general terms, the hydraulic conductivity for unconsolidated sediments tends to increase with increasing grain size and sorting. The velocity of ground water and dissolved contaminants is directly related to the hydraulic conductivity of the saturated zone. Subsurface variations in hydraulic conductivity directly influence contaminant fate and transport by providing preferential pathways for contaminant migration. The most common methods used to quantify hydraulic conductivity in the subsurface are aquifer pumping tests and slug tests. The quantitative analysis of pumping and slug test data is beyond the scope of this document. For information on the quantitative analysis of these data, the reader is referred to the works of Kruseman and de Ridder (1991) and Dawson and Istok (1991).

Table C.3.1 *Representative Values of Hydraulic Conductivity for Various Sediments and Rocks (From Domenico and Schwartz, 1990)*

Material	Hydraulic Conductivity (m/day)	Hydraulic Conductivity (cm/sec)
UNCONSOLIDATED SEDIMENT		
Glacial till	$9 \times 10^{-8} - 2 \times 10^{-1}$	$1 \times 10^{-10} - 2 \times 10^{-4}$
Clay	$9 \times 10^{-7} - 4 \times 10^{-4}$	$1 \times 10^{-9} - 5 \times 10^{-7}$
Silt	$9 \times 10^{-5} - 2$	$1 \times 10^{-7} - 2 \times 10^{-3}$
Fine sand	$2 \times 10^{-2} - 2 \times 10^1$	$2 \times 10^{-5} - 2 \times 10^{-2}$
Medium sand	$8 \times 10^{-2} - 5 \times 10^1$	$9 \times 10^{-5} - 6 \times 10^{-2}$
Coarse sand	$8 \times 10^{-2} - 5 \times 10^2$	$9 \times 10^{-5} - 6 \times 10^{-1}$
Gravel	$3 \times 10^1 - 3 \times 10^3$	$3 \times 10^{-2} - 3$
SEDIMENTARY ROCK		
Karstic limestone	$9 \times 10^{-2} - 2 \times 10^3$	$1 \times 10^{-4} - 2$
Limestone and dolomite	$9 \times 10^{-5} - 5 \times 10^{-1}$	$1 \times 10^{-7} - 6 \times 10^{-4}$
Sandstone	$3 \times 10^{-5} - 5 \times 10^{-1}$	$3 \times 10^{-8} - 6 \times 10^{-4}$
Siltstone	$9 \times 10^{-7} - 1 \times 10^{-3}$	$1 \times 10^{-9} - 1 \times 10^{-6}$
Shale	$9 \times 10^{-9} - 2 \times 10^{-4}$	$1 \times 10^{-11} - 2 \times 10^{-7}$
CRYSTALLINE ROCK		
Vesicular basalt	$3 \times 10^{-2} - 2 \times 10^3$	$4 \times 10^{-5} - 2$
Basalt	$2 \times 10^{-6} - 3 \times 10^{-2}$	$2 \times 10^{-9} - 4 \times 10^{-5}$
Fractured igneous and metamorphic	$7 \times 10^{-4} - 3 \times 10^1$	$8 \times 10^{-7} - 3 \times 10^{-2}$
Unfractured igneous and metamorphic	$3 \times 10^{-9} - 2 \times 10^{-5}$	$3 \times 10^{-12} - 2 \times 10^{-8}$

C.3.1.1.1 Hydraulic Conductivity from Pumping Tests

Pumping tests generally provide the most reliable information about aquifer hydraulic conductivity. Pumping test data for geohydraulic characteristics are most commonly interpreted by graphic techniques. The analytical method used for interpretation of the data will depend upon the physical characteristics of the aquifer and test wells. The assumptions inherent in the analytical method used to calculate aquifer characteristics should be evaluated to ensure acceptance of the method for the subsurface conditions present at the site under investigation.

The interpretation of aquifer pumping test data is not unique. Similar sets of data can be obtained from various combinations of geologic conditions. Field data of drawdown vs. time and/or distance are plotted on graph paper either by hand or using programs such as AQTESOLV® or a spreadsheet program. There are numerous methods of interpreting pumping test data. The method to be used for each pumping test should be selected based on site-specific conditions (aquifer conditions, test conditions, assumptions made, etc.). Most hydrogeology text books contain pumping test evaluation techniques. Two publications dealing with pump test analysis are recommended (Kruseman and de Ridder, 1991 and Dawson and Istok, 1991).

C.3.1.1.2 Hydraulic Conductivity from Slug Tests

Slug tests are a commonly used alternative to pumping tests that are relatively easy to conduct. The biggest advantage of slug tests is that no contaminated water is produced during the test. During pumping tests at fuel-hydrocarbon-contaminated sites, large volumes of contaminated water that must be treated typically are produced. One commonly cited drawback to slug testing is that this method generally gives hydraulic conductivity information only for the area immediately surrounding the monitoring well. If slug tests are going to be relied upon to provide information on the three-dimensional distribution of hydraulic conductivity in an aquifer, multiple slug tests must be performed, both within the same well and at several monitoring wells at the site. It is not advisable to rely on data from one slug test in a single monitoring well. Data obtained during slug testing are generally analyzed using the method of Hvorslev (1951) for confined aquifers or the method of Bouwer and Rice (1976) and Bouwer (1989) for unconfined conditions.

C.3.1.2 Transmissivity

The transmissivity, T , of an aquifer is the product of the aquifer's hydraulic conductivity, K , and the saturated thickness, b :

$$T = Kb \quad \text{eq. C.3.1}$$

For a confined aquifer, b is the thickness of the aquifer between confining units. For unconfined aquifers, b is the saturated thickness of the aquifer measured from the water table to the underlying confining layer. Transmissivity has the units of length squared over time [L^2/T].

C.3.1.3 Hydraulic Head and Gradient

Determining the magnitude of hydraulic gradients is important because gradients influence the direction and rate of contaminant migration. Hydraulic head, H , and specifically, variations in hydraulic head within an aquifer, is the driving force behind ground-water movement and solute migration. The total hydraulic head at one location in a system is the sum of the elevation head, pressure head, and velocity head (Figure C.3.2):

$$H = h_z + h_p + h_v \quad \text{eq. C.3.2}$$

Where:

H = total hydraulic head [L]

h_z = elevation head = z = elevation relative to the reference plane [L]

h_p = pressure head [L]

h_v = velocity head [L]

Pressure head is given by:

$$h_p = \frac{P}{\rho g}$$

Where:

p = fluid pressure

ρ = density

g = acceleration due to gravity

Velocity head is given by:

$$h_v = \frac{v^2}{2g}$$

Where:

v = ground-water velocity

g = acceleration due to gravity

Because h_v is generally assumed to be zero for most ground-water flow, the relationship for total head is generally written:

$$H = z + \frac{P}{\rho g} \quad \text{eq. C.3.3}$$

Thus, the total hydraulic head at a point measured by a piezometer is the sum of the elevation at the base of the piezometer plus the length of the water column in the piezometer. The total hydraulic head in a piezometer is determined by measuring the depth from a surveyed reference point (datum) to the surface of the standing water. The elevation of the water surface is the total hydraulic head in the piezometer. This total head is the total head at the base of the piezometer, not the water table elevation, unless the piezometer terminates immediately below the water table or is a well screened

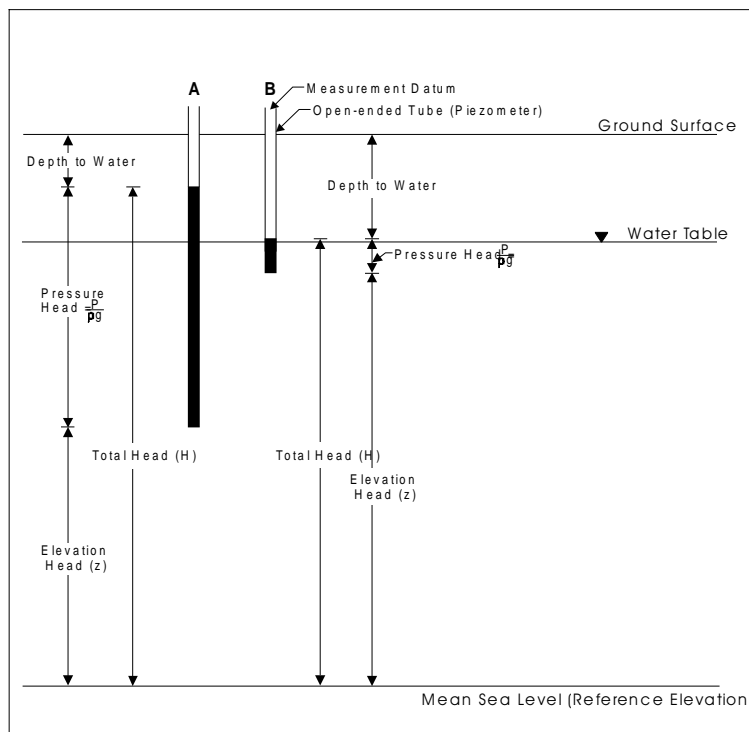


Figure C.3.2 Hydraulic head.

across the water table. Figure C.3.2 shows a pair of nested piezometers that illustrate the relationships between total hydraulic head, pressure head, and elevation head. Because ground water flows from areas with high total head (point A, Figure C.3.2) to areas with lower total head (point B), this figure depicts a water table aquifer with a strong upward vertical gradient. This figure illustrates how nested piezometers (or wells) are used to determine the importance of vertical gradients at a site. This figure also illustrates the importance of using wells screened in the same portion of the aquifer (preferably across the water table) when preparing potentiometric surface maps.

The hydraulic gradient (dH/dL) is a dimensionless number that is the change in hydraulic head (dH) between two points divided by the length of ground-water flow between these same two points, parallel to the direction of ground-water flow, and is given by:

$$\text{Hydraulic Gradient} = \frac{dH}{dL} \quad \text{eq. C.3.4}$$

Where:

dH = change in total hydraulic head between two points [L]

dL = distance between the two points used for head measurement [L]

In a system where flow is not occurring, the total hydraulic head, H , is the same everywhere in the system and the hydraulic gradient is zero. To accurately determine the hydraulic gradient, it is necessary to measure ground-water levels in all monitoring wells at the site. Because hydraulic gradients can change over a short distance within an aquifer, it is essential to have as much site-specific ground-water elevation information as possible so that accurate hydraulic gradient calculations can be made. In addition, seasonal variations in ground-water flow direction can have a profound influence on contaminant transport. To determine the effect of seasonal variations in ground-water flow direction on contaminant transport, quarterly ground-water level measurements should be taken over a period of at least 1 year.

The hydraulic gradient must be determined parallel to the direction of ground-water flow. Unless two monitoring wells screened in the same relative location within the same hydrogeologic unit are located along a line parallel to the direction of ground-water flow, the potentiometric surface map is generally used to determine the hydraulic gradient. To determine the hydraulic gradient, an engineer's scale is used to draw a line perpendicular to the equal-potential lines on the potentiometric surface map (i.e., parallel to the direction of ground-water flow). Measure the distance between the two equal-potential lines, making note of the ground-water potential at each equal-potential line. Subtract the larger potential from the smaller potential, and divide this number by the distance between the two equal potential lines, being sure to use consistent units. The number generated will be a negative number because water flows from areas of higher potential to areas of lower potential.

Example C.3.1: Hydraulic Gradient Calculation

Given the water table elevation map shown in Figure C.3.3, calculate the hydraulic gradient between points A and B. Assume that all wells are screened across the water table.

Solution:

The hydraulic gradient is given by dH/dL . The line connecting points A and B is parallel to the direction of ground-water flow. The water table elevation is 4659.34 ft msl at point A and 4602.41 ft msl at point B. Therefore, because ground water flows from areas of high head to areas of lower head:

$$dH = 4602.41 - 4659.34 = -56.93 \text{ feet}$$

The distance between the two points A and B is 936 feet. Therefore:

$$dL = 936 \text{ feet}$$

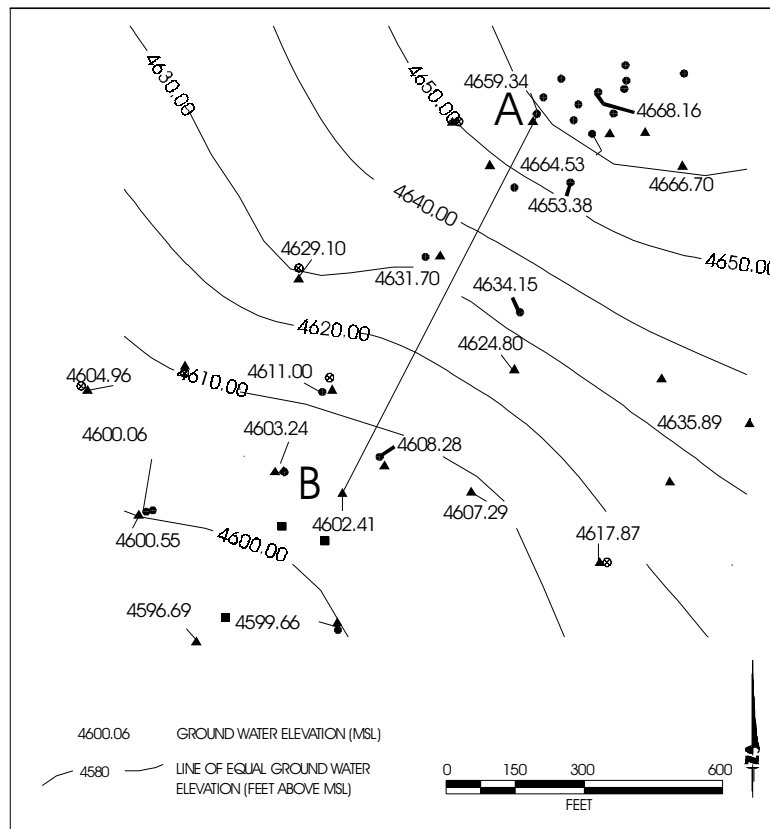


Figure C.3.3 Ground water elevation map.

and

$$\frac{dH}{dL} = \frac{-56.93 \text{ ft}}{936 \text{ ft}} = -9.06 \frac{\text{ft}}{\text{ft}} = -0.06 \frac{m}{m}$$

C.3.1.4 Total Porosity (n) and Effective Porosity (n_e)

Total porosity (n) is the volume of voids in a unit volume of aquifer. Specific retention is the amount of water (volumetric) that is retained against the force of gravity after a unit volume of an unconfined aquifer is drained. Storativity is defined as the volume of water that a confined aquifer takes into or releases from storage per unit surface area of the aquifer per unit change in total hydraulic head. Effective porosity, n_e , is the total porosity of the aquifer minus the specific retention (unconfined) or storativity (confined) of the aquifer:

$$n_e = n - S \quad \text{eq. C.3.5}$$

Where:

n_e = effective porosity [dimensionless]

n = total porosity [dimensionless]

S = specific retention (unconfined) or storativity (confined) [dimensionless]

Effective porosity can be estimated using the results of a tracer test. Although this is potentially the most accurate method, time and monetary constraints can be prohibitive. For this reason, the most common technique is to use an accepted literature value for the types of materials making up the aquifer matrix, and then to calibrate a contaminant transport model by adjusting the value of effective porosity (in conjunction with other input parameters such as transmissivity) within the range of

accepted literature values until the modeled and observed contaminant distribution patterns match. Because aquifer materials can have a range of effective porosity, sensitivity analyses should be performed to determine the effect of varying the effective porosity on numerical model results. Values of effective porosity chosen for the sensitivity analyses should vary over the accepted range for the aquifer matrix material. Table C.3.2 presents accepted literature values for total porosity and effective porosity.

Table C.3.2 *Representative Values of Dry Bulk Density, Total Porosity, and Effective Porosity for Common Aquifer Matrix Materials (After Walton, 1988 and Domenico and Schwartz, 1990)*

Aquifer Matrix	Dry Bulk Density (gm/cm³)	Total Porosity	Effective Porosity
Clay	1.00-2.40	0.34-0.60	0.01-0.2
Peat	---	---	0.3-0.5
Glacial Sediments	1.15-2.10	---	0.05-0.2
Sandy Clay	---	---	0.03-0.2
Silt	---	0.34-0.61	0.01-0.3
Loess	0.75-1.60	---	0.15-0.35
Fine Sand	1.37-1.81	0.26-0.53	0.1-0.3
Medium Sand	1.37-1.81	---	0.15-0.3
Coarse Sand	1.37-1.81	0.31-0.46	0.2-0.35
Gravelly Sand	1.37-1.81	---	0.2-0.35
Fine Gravel	1.36-2.19	0.25-0.38	0.2-0.35
Medium Gravel	1.36-2.19	---	0.15-0.25
Coarse Gravel	1.36-2.19	0.24-0.36	0.1-0.25
Sandstone	1.60-2.68	0.05-0.30	0.1-0.4
Siltstone	---	0.21-0.41	0.01-0.35
Shale	1.54-3.17	0.0-0.10	---
Limestone	1.74-2.79	0.0-50	0.01-0.24
Granite	2.24-2.46	---	---
Basalt	2.00-2.70	0.03-0.35	---
Volcanic Tuff	---	---	0.02-0.35

C.3.1.5 Linear Ground-water Flow Velocity (Seepage or Advective Velocity)

The average linear ground-water flow velocity (seepage velocity) in one dimension in the direction parallel to ground-water flow in a saturated porous medium is given by:

$$v_x = \frac{K}{n_e} \frac{dH}{dL} \quad \text{eq. C.3.6}$$

Where:

v_x = average linear ground-water velocity parallel to ground-water flow direction (seepage velocity) [L/T]

K = hydraulic conductivity [L/T]

n_e = effective porosity [L³/L³]

$\frac{dH}{dL}$ = hydraulic gradient [L/L]

The average linear ground-water flow velocity should be calculated to estimate ground-water flow and solute transport velocity, to check the accuracy of ground-water models, and to calculate first-order biodegradation rate constants.

Example C.3.2: Linear Ground-water Flow Velocity Calculation

Calculate the linear ground-water flow velocity in a medium-grained sandy aquifer. The hydraulic gradient as determined from the potentiometric surface map in the previous example is -0.06 m/m. The hydraulic conductivity is 1.7×10^{-1} m/day as determined by pumping tests.

Solution:

Because the effective porosity of this sediment is not known, it is necessary to estimate this parameter. From Table C.3.2, the effective porosity for a medium-grained sand is approximately 23 percent.

$$v_x = -\frac{K}{n_e} \frac{dH}{dL} = -\frac{(0.17 \text{ m/day})(-0.06 \text{ m/m})}{0.23} = 0.044 \text{ m/day}$$

C.3.1.6 Coefficient of Retardation and Retarded Contaminant Transport Velocity

When the average linear velocity of a dissolved contaminant is less than the average linear velocity of the ground water, the contaminant is said to be “retarded.” The difference between the velocity of the ground water and that of the contaminant is caused by sorption and is described by the coefficient of retardation, R , which is defined as:

$$R = \frac{v_x}{v_c} \quad \text{eq. C.3.7}$$

Where:

R = coefficient of retardation

v_x = average linear ground-water velocity parallel to ground-water flow

v_c = average velocity of contaminant parallel to groundwater flow

The ratio v_x/v_c describes the relative velocity between the ground water and the dissolved contaminant. When $K_d = 0$ (no sorption), the transport velocities of the ground water and the solute are equal ($v_x = v_c$). If it can be assumed that sorption is adequately described by the distribution coefficient, the coefficient of retardation for a dissolved contaminant (for saturated flow) is given by:

$$R = 1 + \frac{\rho_b K_d}{n} \quad \text{eq. C.3.8}$$

Where:

R = coefficient of retardation

ρ_b = bulk density (Section C.3.1.6.1)

K_d = distribution coefficient (Section C.3.1.6.2)

n = total porosity

This relationship expresses the coefficient of retardation in terms of the bulk density and effective porosity of the aquifer matrix and the distribution coefficient for the contaminant. Substitution of this equation into equation C.3.7 gives:

$$\frac{v_x}{v_c} = 1 + \frac{\rho_b K_d}{n} \quad \text{eq. C.3.9}$$

Solving for the contaminant velocity, v_c , gives:

$$v_c = \frac{v_x}{1 + \frac{\rho_b K_d}{n}} \quad \text{eq. C.3.10}$$

Retardation of a contaminant relative to the advective transport velocity of the ground-water flow system has important implications for natural attenuation. If retardation is occurring, dissolved oxygen and other electron acceptors traveling at the advective transport velocity of the ground water sweep over the contaminant plume from the upgradient margin. This results in greater availability of electron acceptors within the plume for biodegradation of fuel hydrocarbons. In addition, adsorption of a contaminant to the aquifer matrix results in dilution of the dissolved contaminant plume.

C.3.1.6.1 Bulk Density

The bulk density of a soil, ρ_b , as used in most ground-water models, expresses the ratio of the mass of dried soil to its total volume (solids and pores together).

$$\rho_b = \frac{M_s}{V_T} = \frac{M_s}{(V_s + V_a + V_w)} \quad \text{eq. C.3.11}$$

Where:

- ρ_b = bulk density
- M_s = mass of solid in the system
- V_T = total volume in the system
- V_s = volume of solid in the system
- V_a = volume of air (or gas) in the system
- V_w = volume of water (or liquid) in the system

Bulk density is related to particle density by:

$$\rho_b = (1 - n)\rho_s \quad \text{eq. C.3.12}$$

Where:

- ρ_b = bulk density
- n = total porosity
- ρ_s = density of grains comprising the aquifer

The bulk density is always less than the particle density, ρ_s ; for example, if pores constitute half the volume, then ρ_b is half of ρ_s . The bulk density of a soil is affected by the structure of the soil (looseness and degree of compaction), as well as by its swelling and shrinking characteristics, both of which depend on clay content and soil moisture. Even in extremely compacted soil, the bulk density remains appreciably lower than the particle density. This is because the particles can never interlock perfectly, and the soil remains a porous body, never completely impervious. In sandy soils, ρ_b can be as high as 1.81 gm/cm³. In aggregated loams and clayey soils, ρ_b can be as low as 1.1gm/cm³. Table C.3.2 contains representative values of dry bulk density for common sediments and rocks.

C.3.1.6.2 Distribution Coefficient and Total Organic Carbon Content

The distribution coefficient is described in Section B.4.3. Recall equation B.4.10, which gives the relationship between f_{oc} and K_{oc} :

$$K_d = K_{oc} f_{oc} \quad \text{eq. C.3.13}$$

Where:

K_d = distribution coefficient [L^3/M]

K_{oc} = soil adsorption coefficient for soil organic carbon content [L^3/M]

f_{oc} = fraction soil organic carbon (mg organic carbon/mg soil) [M/M]

Representative K_{oc} values are given in Table B.4.1. The fraction of soil organic carbon must be determined from site-specific data. Representative values of total organic carbon (TOC) in common sediments are given in Table C.3.3. Because most solute transport occurs in the most transmissive aquifer zones, it is imperative that soil samples collected for total organic carbon analyses come from these zones in background areas. To be conservative, the average of all total organic carbon concentrations from sediments in the most transmissive aquifer zone should be used for retardation calculations.

Table C.3.3 Representative Values of Total Organic Carbon for Common Sediments

Texture	Depositional Environment	Fraction Organic Carbon	Site Name
medium sand	fluvial-deltaic	0.00053 - 0.0012	Hill AFB, Utah
fine sand		0.0006 - 0.0015	Bolling AFB, D.C.
fine to coarse sand	back-barrier (marine)	0.00026 - 0.007	Patrick AFB, Florida
organic silt and peat	glacial (lacustrine)	0.10 - 0.25	Elmendorf AFB, Alaska
silty sand	glaciofluvial	0.0007 - 0.008	Elmendorf AFB, Alaska
silt with sand, gravel and clay (glacial till)	glacial moraine	0.0017 - 0.0019	Elmendorf AFB, Alaska
medium sand to gravel	glaciofluvial	0.00125	Elmendorf AFB, Alaska
loess (silt)	eolian	0.00058 - 0.0016	Offutt AFB, Nebraska
fine - medium sand	glaciofluvial or glaciolacustrine	< 0.0006 - 0.0061	Truax Field, Madison Wisconsin
fine to medium sand	glaciofluvial	0.00021 - 0.019	King Salmon AFB, Fire Training Area, Alaska
			Dover AFB, Delaware
fine to coarse sand	glaciofluvial	0.00029 - 0.073	Battle Creek ANGB, Michigan
sand	fluvial	0.0057	Oconee River, Georgia ^{a/}
coarse silt	fluvial	0.029	Oconee River, Georgia ^{a/}
medium silt	fluvial	0.020	Oconee River, Georgia ^{a/}
fine silt	fluvial	0.0226	Oconee River, Georgia ^{a/}
silt	lacustrine	0.0011	Wildwood, Ontario ^{b/}
fine sand	glaciofluvial	0.00023 - 0.0012	Various sites in Ontario ^{b/}
medium sand to gravel	glaciofluvial	0.00017 - 0.00065	Various sites in Ontario ^{b/}

a/ Karickhoff, 1981•

b/ Domenico and Schwartz (1990)•

Example C.3.3: Retarded Solute Transport Velocity Calculation

For ground-water flow and solute transport occurring in a shallow, saturated, well-sorted, fine-grained, sandy aquifer, with a total organic carbon content of 0.7 percent, a hydraulic gradient of - 0.015 m/m, and an hydraulic conductivity of 25 m/day, calculate the retarded contaminant velocity for trichloroethene.

Solution:

Because the total porosity, effective porosity, and the bulk density are not given, values of these parameters are obtained from Table C.3.2. The median values for total porosity, effective

porosity, and bulk density are approximately 0.4, 0.2, and 1.6 kg/L, respectively.

The first step is to calculate the average linear ground-water velocity, v_x .

$$v_x = -\frac{(25 \text{ m/day})(-0.015 \text{ m/m})}{0.2} = 1.9 \text{ m/day}$$

The next step is to determine the distribution coefficient, K_d . Values of K_{oc} for chlorinated solvents and BTEX are obtained from Tables B.2.1 and B.2.2, respectively, and are listed in Table C.3.4.

For trichloroethene $K_{oc} = 87 \text{ L/kg}$, and (using equation C.3.13):

$$K_d = \left(87 \frac{\text{L}}{\text{kg}}\right)(0.007) = 0.61 \frac{\text{L}}{\text{kg}}$$

The retarded contaminant velocity is given by (equation C.3.10):

$$v_c = \frac{1.9 \text{ m/day}}{1 + \frac{(1.6 \text{ kg/L})(0.61 \text{ L/kg})}{0.4}} = 0.55 \text{ m/day}$$

Table C.3.4 presents the estimated coefficient of retardation contaminant velocity for a number of contaminants under the conditions of Example C.3.3. This example illustrates that contaminant sorption to total organic carbon can have a profound influence on contaminant transport by significantly slowing the rate of dissolved contaminant migration.

Table C.3.4 Example Retardation Calculations for Select Compounds

Compound	K_{oc} L/kg	Fraction Organic Carbon	Distribution Coefficient (L/kg)	Bulk Density (kg/L)	Total Porosity	Coefficient of Retardation	Advective Ground-water Velocity (m/day)	Contaminant Velocity (m/day)
Benzene	79	0.007	0.553	1.60	0.40	3.21	1.90	0.59
Toluene	190	0.007	1.33	1.60	0.40	6.32	1.90	0.30
Ethylbenzene	468	0.007	3.276	1.60	0.40	14.10	1.90	0.13
m-xylene	405	0.007	2.835	1.60	0.40	12.34	1.90	0.15
Tetrachloroethene	209	0.007	1.463	1.60	0.40	6.85	1.90	0.28
Trichloroethene	87	0.007	0.609	1.60	0.40	3.44	1.90	0.55
cis-1,2-Dichloroethene	49	0.007	0.343	1.60	0.40	2.37	1.90	0.80
Vinyl Chloride	2.5	0.007	0.0175	1.60	0.40	1.07	1.90	1.78
1,3,5-trimethylbenzene	676	0.007	4.732	1.60	0.40	19.93	1.90	0.10

C.3.2 CONTAMINANT SOURCE TERM CALCULATIONS

NAPLs present in the subsurface represent a continuing source of ground-water contamination. NAPLs may be made up of one compound, or more likely, a mixture of compounds. Concentrations of dissolved contaminants and the lifetime of NAPL source areas and associated ground-water plumes are ultimately determined by the rate at which contaminants dissolve from the NAPL. When sufficient quantities of NAPL are present, the unsaturated zone may initially be saturated with

NAPL, and the NAPL may migrate under the influence of gravity. After a period of time the NAPL may drain from the pores under the influence of gravity, leaving a thin coating of NAPL. Depending on the surface area of the subsurface materials, the surface tension of the NAPL, and the porosity and permeability of the subsurface materials, some NAPL also may be held between the grains by capillarity. NAPL adhering to the grains of the aquifer matrix or retained by capillarity is herein referred to as residual NAPL. In residual zones, NAPL will be present in immobile blobs or ganglia that may occupy 10 percent or less of the pore space (Feenstra and Guiguer, 1996). If the NAPL is at saturation and is mobile within and among the pores of the aquifer matrix, the NAPL is referred to as mobile NAPL. Mobile NAPL may occupy as much as 50 to 70 percent of the pore space and can reduce flow of water through these zones.

In the unsaturated zone, dissolution from residual or mobile NAPL into downward-migrating precipitation (recharge) will occur, as well as migration and dissolution of vapors. In the saturated zone, dissolution of contaminants from residual NAPL occurs as ground-water flows through the residual zone. Dissolution from mobile NAPL mostly takes place along the tops, bottoms, or lateral margins of the NAPL bodies, because ground-water (or recharge) flow through the NAPL is restricted. Because the distribution of residual NAPL results in a greater surface area of product in contact with ground water and does not restrict ground-water velocities, concentrations of contaminants entering ground water will typically be closer to the compounds' equilibrium solubilities than in the case of mobile NAPL bodies. The equilibrium solubility of the compound(s) of interest will depend on the composition of the NAPL (i.e., the molar fraction of the NAPL represented by the compound).

In general, residual and mobile NAPL may be present above or below the water table, but direct dissolution into ground water will only occur when NAPL is at or below the capillary fringe. In either case, quantifying the flux of contamination entering ground water from above or below the water table is a difficult proposition. The processes governing dissolution from NAPLs are complex and depend upon many variables (Feenstra and Guiguer, 1996). Among these variables (in the saturated zone) are the shape of a mobile NAPL body, the contact area between the NAPL and the ground water, the velocity of the ground water moving through or past the NAPL, the effect of residual NAPL on the effective porosity of the contact zone, the solubility of the compounds of interest, the relative fractions of the compounds in the NAPL, the diffusion coefficients of the compounds, and the effects of other compounds present in the NAPL. This will be further complicated by any processes in the vadose zone (e.g., volatilization, dissolution from residual NAPL into recharge, or dissolution of vapors into recharge) that also will add contaminant mass to ground water. Further, as the mass of the NAPL body changes over time, the rate of dissolution will also change. Clearly, given the number of variables that affect the transfer of contaminant mass to ground water, it is difficult to accurately estimate the flux of contaminants into ground water. Depending on the intended use of the flux estimate, different approaches can be used.

If one desires to estimate a source term for a contaminant fate and transport model, one can attempt to estimate the mass loading rate and use that estimate as an input parameter. However, this often does not yield model concentrations (dissolved) that are similar to observed concentrations. As a result, the source in the model often becomes a calibration parameter (Mercer and Cohen, 1990; Spitz and Moreno, 1996). This is because the effects of the source (i.e., the dissolved contaminant plume) are easier to quantify than the actual flux from the source. The frequent need for such a "black box" source term has been borne out during modeling associated with evaluations of natural attenuation of fuel hydrocarbons [following the AFCEE technical protocol (Wiedemeier *et al.*, 1995d)] at over 30 U.S. Air Force sites. Use of other methods to calculate source loading for those models often produced model concentrations that differed from observed concentrations by as

much as an order of magnitude. From the model, the flux estimate then can be used for estimating source lifetimes or other such calculations.

For other purposes, one can estimate flux using several methods, as summarized by Feenstra and Guiguer (1996). For bodies of mobile LNAPL, this is more practical, because the area of NAPL in contact with ground water can be estimated from plume/pool dimensions. Where most NAPL is residual, the surface area can be highly variable, and cannot be measured in the field. Laboratory studies to understand and quantify mass transfer from residual NAPL in porous media are in the early stages, and when such mass transfer is modeled, surface area is a calibration parameter with great uncertainty (Abriola, 1996). Most methods of estimating NAPL dissolution rates require an estimate of the contact area and, therefore, will contain a great deal of uncertainty. This is one of the main reasons why, for purposes of modeling, the “black box” source term is more commonly used.

One reason practitioners want to estimate mass transfer rates is to provide a basis for estimating contaminant source lifetimes, which can affect regulatory decisions and remedial designs. To determine how long it will take for a dissolved contaminant plume to fully attenuate, it is necessary to estimate how fast the contaminants are being removed from the NAPL. In general, it is difficult to estimate cleanup times, so conservative estimates should be made based on NAPL dissolution rates. Predicting the cleanup time for sites with mobile NAPL is especially difficult because residual NAPL will remain after the recoverable mobile NAPL has been removed. Of course, this is all complicated by the many factors that affect dissolution rates as discussed above. Moreover, most methods do not account for changing dissolution rates as a result of NAPL volume loss (and subsequent surface area decrease), preferential partitioning from mixed NAPLs, and the change in porosity (and, therefore, ground-water velocity) resulting from NAPL dissolution. Finally, the mass of the NAPL present in the subsurface must also be estimated, lending further uncertainty to any calculation of source lifetime.

There are several ways to quantify the mass loading rate from a body of mobile or residual NAPL. Feenstra and Guiguer (1996) present a good summary of some common methods. As noted above, transfer rates calculated from these methods are all dependent upon several parameters, many of which cannot be measured or derived from the literature. This is especially true for residual NAPL. Johnson and Pankow (1992) present a method for estimating dissolution rates from pools of NAPL which contact ground water over an area that is essentially two-dimensional. Many other dissolution models may be available; however, as noted before, the experimental evidence to support dissolution models is really just starting to be collected. Despite these limitations, some of these models can prove useful, and a selected few are presented (in limited detail) in the following subsections.

If estimating mass flux rates is less important, one can use direct measurement or equilibrium concentration calculations to estimate contaminant source area concentrations. The first method involves directly measuring the concentration of dissolved contaminants in ground water near the NAPL plume. The second method involves the use of partitioning calculations. These approaches are described in the following sections. This type of data can be useful if it can be demonstrated that the source is not capable of introducing concentrations of compounds of concern that exceed regulatory limits, or that with slight weathering the same results can be expected. Source area concentrations, whether measured or calculated, also may be used to provide calibration targets for transport models in which a “black box” source term is used.

If contaminant concentrations in the residual and mobile NAPL are not decreasing over time, or if they are decreasing very slowly, extremely long times will be required for natural attenuation of the dissolved contaminant plume. This will likely make natural attenuation less feasible and will reduce the chance of implementation. In order for natural attenuation to be a viable remedial option, the

source of continuing ground-water contamination must be decreasing over time (decaying), either by natural weathering processes or via engineered remedial solutions such as mobile NAPL recovery, soil vapor extraction, bioventing, or bioslurping. Because natural weathering processes can be fairly slow, especially in systems where the NAPL dissolves slowly or is inhibited from volatilizing or biodegrading, it will generally be necessary to implement engineered remedial solutions to remove the NAPL or reduce the total mass of residual and dissolved NAPL.

A discussion of estimating source terms for sites contaminated solely with fuel hydrocarbons is presented by Wiedemeier *et al.* (1995a). In general, estimating dissolution rates of individual compounds from fuels is simpler than estimating rates of dissolution from other NAPL mixtures because there is a great deal of experimental evidence regarding partitioning and equilibrium solubilities of individual compounds from common fuel mixtures. Methods presented in the following subsections can use such data to reduce some of the uncertainty in source term calculations.

Typical uses of chlorinated solvents (e.g., degreasing or parts cleaning) and past disposal practices that generally mixed different waste solvents or placed many types of waste solvents in close proximity have resulted in complex and greatly varying NAPL mixtures being released at sites. For mixtures containing other compounds (e.g., either DNAPLs containing multiple chlorinated compounds, or fuel LNAPLs containing commingled chlorinated compounds), the equilibrium solubility of the individual compounds of interest must first be calculated, then that information can be used in the common mass transfer rate calculations. Except in the case of pure solvent spills, therefore, the estimation of dissolution rates is then further complicated by this need to estimate equilibrium solubilities from the mixture.

Because this work focuses largely on saturated-zone processes, vadose zone dissolution processes will not be discussed in any detail. However, this discussion will provide a starting point for estimating source terms for ground-water contaminant fate and transport modeling, as well as for estimating source and plume lifetimes. As a starting point, two basic methods of estimating or measuring equilibrium dissolved contaminant concentrations in the vicinity of NAPL bodies are presented. In addition, methods for estimating fluxes summarized by Feenstra and Guiguer (1996) and presented by Johnson and Pankow (1992) will be briefly summarized.

C.3.2.1 Direct Measurement of Dissolved Contaminant Concentrations in Ground Water in Contact with NAPL

Two methods can be used to determine the dissolved concentration of contaminants in ground water near a NAPL plume. The first method involves collecting ground-water samples from near a NAPL lens in monitoring wells. The second method involves collecting samples of mixed NAPL and water from monitoring wells.

C.3.2.1.1 Collecting Ground-water Samples from Near the NAPL

This method involves carefully sampling ground water beneath a floating LNAPL lens or near a DNAPL lens. One way of collecting a ground-water sample from beneath a lens of floating LNAPL or above/adjacent to a DNAPL body involves using a peristaltic pump. For LNAPL, the depth to the base of the mobile LNAPL is measured, a length of high-density polyethylene (HDPE) tubing that will reach 1 to 2 feet beneath the LNAPL is lowered into the well, and the sample is collected. For DNAPL, the tube would be cut to reach 1 to 2 feet above the NAPL. Another useful technique for obtaining such samples where the depth to ground water is too deep to allow use of a peristaltic pump is to use a Grundfos® pump. If a Grundfos® pump is used to collect a water sample from beneath LNAPL, it is imperative that the pump be thoroughly cleaned after each use, and that good sampling logic be used (e.g., sample less contaminated wells first). Also, dedicated bladder pumps that are being used for long-term monitoring (LTM) in wells with NAPL can be used to collect water samples from beneath or above the NAPL.

C.3.2.1.2 Collecting Mixed Ground-water/NAPL Samples

This method involves collecting a sample of ground water and NAPL from a monitoring well, placing the sample in a sealed container used for volatile organics analysis being careful to ensure there is no headspace, allowing the sample to reach equilibrium, and submitting the water above or below the floating NAPL to a qualified laboratory for analysis. A disposable bailer generally works best for collection of this type of sample. Smith *et al.* (1981) has information on how to conduct such a test for LNAPL. Two or three samples should be collected from different monitoring wells containing NAPL at the site. This test should only be done when it is not possible to collect a discrete sample from above or below the NAPL.

C.3.2.2 Equilibrium Partitioning Calculations

The NAPL present at a site represents a continuing source of contamination because chlorinated solvents, BTEX, and other compounds will partition from the NAPL into the ground water. In such cases, it is generally necessary to estimate the dissolved concentration of contaminants expected in ground water near the LNAPL. Partitioning calculations can be performed for sites with NAPL to quantify contaminant loading from the NAPL into the ground water at the time the ground water or NAPL samples are collected. Such calculations allow a crude estimation of the impact of continuing sources of contamination on dissolved contaminant concentrations. The results of partitioning calculations may show that even if the NAPL is allowed to remain in the ground, dissolved contaminant concentrations will remain below regulatory guidelines. This is especially true when weathered NAPLs with initially low contaminant concentrations are present. Partitioning calculations made by Wiedemeier *et al.* (1993) showed that NAPL present in the subsurface at a fueling facility near Denver, Colorado, was incapable of producing dissolved contaminant concentrations in ground water above regulatory standards. Such partitioning calculations should be confirmed with an LTM program.

On the other hand, if partitioning calculations indicate that continued dissolution will produce contaminant concentrations exceeding regulatory guidelines, further work will be needed. The contaminant concentrations calculated by equilibrium methods will clearly not provide mass flux estimates that can be used in modeling; again, the “black box” methods will be more useful. Moreover, there is no estimation of the actual mass flux across the entire body of NAPL and, therefore, source lifetimes and weathering rates cannot be estimated directly from partitioning data. More advanced calculations, such as those that will be discussed in later sections, are then required, keeping in mind that greater uncertainties will be introduced.

When found in the saturated zone, residual NAPL is extremely difficult to remove. Maximum contaminant concentrations resulting from such partitioning will occur when the ground water and NAPL reach equilibrium. Assuming that equilibrium is reached gives the most conservative modeling results.

C.3.2.2.1 Equilibrium Partitioning of Contaminants from Mobile NAPL into Ground Water

Because most NAPLs will be a mixture of compounds, the solubilities of those compounds will be lower than the solubility of the individual compound (which is what is most commonly found in the literature). For an organic NAPL mixture, the dissolved concentration of each compound (in equilibrium with the mixture) can be approximated by:

$$C_{sat,m} = X_m C_{sat,p} \quad \text{eq. C.3.14}$$

Where:

$C_{sat,m}$ = solubility of compound from mixture

X_m = mole fraction of compound in the mixture

$C_{sat,p}$ = solubility of pure compound

This equilibrium concentration may also be referred to as the effective solubility of the compound from the mixture. Experimental evidence (Banerjee, 1984; Broholm and Feenstra, 1995) have suggested that eq. C.3.14 produces reasonable approximations of effective solubilities for mixtures of structurally similar compounds, and that the relationship works best for binary mixtures of similar compounds. For other mixtures, the error is greater due to the complex solubility relationships created; however, the method is appropriate for many environmental studies for which there are many other uncertainties (Feenstra and Guiguer, 1996).

For complex mixtures (e.g., multiple identified and unidentified solvents, or mixed fuels and solvents), it will be necessary to estimate the weight percent and an average molecular weight of the unidentified fraction of the NAPL before the calculation can be completed. In doing so, it should be remembered that increasing the average molecular weight for the unidentified fraction will produce greater estimated effective solubilities for the identified contaminants. A higher molecular weight for the unidentified fraction will result in a lower mole fraction for that fraction and, therefore, higher mole fractions (and solubilities) for the known compounds. Feenstra and Guiguer (1996) provide an example of these calculations for a mixture of chlorinated and nonchlorinated compounds.

In the case of fuel hydrocarbon mixtures, experimental partitioning data has been collected and used to develop individual-compound solubility calculations, largely because fuel mixtures are somewhat consistent in their makeup. The fuel-water partitioning coefficient, K_{fw} , is defined as the ratio of the concentration of a compound in the fuel to the compound's equilibrium concentration in water in contact with the fuel:

$$K_{fw} = \frac{C_f}{C_w} \quad \text{eq. C.3.15}$$

Where:

K_{fw} = fuel-water partitioning coefficient [dimensionless]

C_f = concentration of the compound in the fuel [M/L³]

C_w = concentration of the compound dissolved in ground water [M/L³]

A summary of values of K_{fw} for BTEX and trimethylbenzenes (TMB) in jet fuel and gasoline are presented by Wiedemeier *et al.* (1995d), along with the relationships relating K_{fw} to the aqueous solubility of a pure compound in pure water, S , which can be used to estimate K_{fw} for compounds for which there is no experimental data.

Using the definition of K_{fw} presented above, the maximum (equilibrium) total dissolved BTEX concentration resulting from the partitioning of BTEX from NAPL into ground water is given by:

$$C_w = \frac{C_f}{K_{fw}} \quad \text{eq. C.3.16}$$

This relationship predicts the concentration of dissolved BTEX in the ground water if the LNAPL is allowed to remain in contact with the ground water long enough so that equilibrium between the two phases is reached. Further discussion and example calculations for this method are presented by Wiedemeier *et al.* (1995d).

C.3.2.3 Mass Flux Calculations

In general, the rate of mass transfer from a NAPL can be given as the product of a mass transfer coefficient, a concentration difference, and a contact area. As Feenstra and Guiguer (1996) note, the driving force for mass transfer is the concentration difference across a boundary layer between the NAPL and the ground water. The concentration difference can be approximated using the effective solubility of a compound (eq. C.3.14) and either the measured concentration of the compound in ground water adjacent to the NAPL, or a calculated (theoretical) ground-water concentration. How-

ever, the contact area and the mass transfer coefficient incorporate a great deal of uncertainty and are typically calibration parameters for modeling dissolution, as discussed previously.

Once these parameters have been estimated, one can use them in a variety of models. In general, models for dissolution of NAPL in porous media either assume local equilibrium between phases, or assume that dissolution is a first-order process governed by the variables discussed above (Feenstra and Guiguer, 1996). Abriola and Pinder (1985a), Baehr and Corapcioglu (1987), and Kaluarachchi and Parker (1990) developed two-dimensional NAPL migration models that account for dissolution using the local equilibrium assumption (LEA). As noted by Abriola (1996), these studies generally were computer modeling studies for which follow-up laboratory work is ongoing and uncovering additional factors to consider. For single-component NAPLs, models utilizing a first-order reaction have been developed by Miller *et al.* (1990), Powers *et al.* (1992), Brusseau (1992), Guiguer (1993), and Guiguer and Frind (1994). For multi-component NAPLs, a model developed by Shiu *et al.* (1988) and Mackay *et al.* (1991) may be of use.

Due to approximate nature of flux calculations and the inherent uncertainty in those calculations, we have chosen to omit a detailed discussion of such efforts. The numerical modeling using LEA methods is beyond the scope of this work, and may not be practical for use at most sites. Instead, we will present a brief review of ideas presented by Feenstra and Guiguer (1996) and Johnson and Pankow (1992) in order to illustrate some of the concepts involved in estimating flux terms. Should further detail or other methods be desired, both of those works provide excellent background and references to start with, including many of the works referenced in this discussion of source term calculations.

C.3.2.3.1 General Mass Transfer Models

Using concepts from the field of chemical engineering, Feenstra and Guiguer (1996) note that for a single-component NAPL, simple dissolution of the compound may be described by:

$$N = K_c (C_w - C_{sat}) \quad \text{eq. C.3.17}$$

Where:

- N = flux of the species of interest (M/L²T)
- K_c = mass transfer coefficient (L/T)
- C_w = concentration of compound in bulk aqueous phase (M/L³)
- C_{sat} = concentration of compound at NAPL-water interface (taken as the solubility of the compound) (M/L³)

The mass transfer coefficient may be calculated various ways, but in all cases, the diffusivity of the species of interest is a factor. Feenstra and Guiguer (1996) present three methods for determining a mass transfer coefficient.

In a porous media, the mass transfer rate per volume of porous medium can be defined by multiplying the mass flux by the ratio of NAPL surface contact area to the unit volume of porous medium, yielding:

$$N^* = \lambda (C_w - C_{sat}) \quad \text{eq. C.3.18}$$

Where:

- N^* = flux of the species of interest per unit volume of porous medium (M/L²T)
- λ = lumped mass transfer coefficient (L/T)
- C_w = concentration of compound in bulk aqueous phase (M/L³)
- C_{sat} = concentration of compound at NAPL-water interface (taken as the solubility of the compound) (M/L³)

The lumped mass transfer coefficient is the product of K_c and the ratio of the NAPL surface contact

area and the unit volume of the porous media. This can further be extended for multicomponent NAPLs :

$$N_m^* = \lambda_m (C_{w,m} - C_{sat,m}) \quad \text{eq. C.3.19}$$

Where:

N_m^* = flux of component m per unit volume of porous medium (M/L²T)

λ_m = lumped mass transfer coefficient for component m (L/T)

$C_{w,m}$ = concentration of component m in bulk aqueous phase (M/L³)

$C_{sat,m}$ = concentration of component m at NAPL-water interface (calculated using eq. C.3.14) (M/L³)

Further complicating all of these relationships is the fact that as dissolution continues, λ_m will vary over time as the amount of NAPL changes. This can be accounted by using the following first-order relation:

$$N_m = S_w \lambda_m (C_{sat,m} - C_{w,m}) \quad \text{eq. C.3.20}$$

Where:

N_m = flux of component m per unit volume of porous medium (M/L²T)

S_w = average fraction of pore volume occupied by water

λ_m = lumped mass transfer coefficient for component m (L/T)

$C_{w,m}$ = concentration of component m in bulk aqueous phase (M/L³)

$C_{sat,m}$ = concentration of component m at NAPL-water interface (calculated using eq. C.3.14)) (M/L³)

Again, it bears repeating that on the field scale, measurement of many of the parameters used for these calculations is not possible, and, therefore, great uncertainty is introduced. Source terms calculated using these or any other methods should be presented in that light, and if used for solute transport modeling, should be accompanied with a sensitivity analysis.

C.3.2.3.2 Nonequilibrium Partitioning Model of Johnson and Pankow (1992)

The steady-state, two-dimensional dissolution of contaminants from a pool of NAPL floating on the water table into ground water (assumed to be a semi-infinite medium) can be described by the steady-state, two-dimensional, advection-dispersion equation (Hunt *et al.*, 1988):

$$v_x \frac{\partial C}{\partial x} = D_z \frac{\partial^2 C}{\partial z^2} \quad x, z > 0 \quad \text{eq. C.3.21}$$

Where:

C = contaminant concentration dissolved in water

v_x = average linear ground-water velocity

D_z = vertical dispersion coefficient

If it is assumed that:

- The time required for total NAPL dissolution is exceedingly long in comparison to the contact time between the NAPL pool and the flowing ground water
- The NAPL pool is wide compared to the horizontal transverse mixing process
- The NAPL pool can be approximated as a rectangle
- The NAPL lens width does not affect the dissolution rate
- The elevation of the NAPL lens is taken as $z=0$, with z measured positively upward
- The boundary conditions are:

$$\begin{aligned} C(x, z = 0) &= 0 \\ C(x, z = 0) &= C_e \quad 0 \leq x \leq L \\ C(x = 0, z) &= 0 \end{aligned}$$

Where:

- C = contaminant concentration dissolved in water
- C_e = effective water solubility
- L = horizontal length of NAPL pool

then the rate of dissolution of constituents from an LNAPL lens into ground water flowing beneath the lens can be calculated as two-dimensional, steady-state dissolution, and the surface area averaged mass transfer rate, M_a , is calculated as (Johnson and Pankow, 1992; Hunt *et al.*, 1988):

$$M_a = C_e n_e \sqrt{\frac{4 D_z v_x}{\pi L}} \quad \text{eq. C.3.22}$$

Where:

- n_e = effective porosity
- L = length of NAPL lens parallel to ground-water flow direction
- v_x = average linear ground-water flow velocity
- C_e = effective water solubility (proportional to a compound's pure phase solubility and mole fraction in the NAPL)
- D_z = vertical dispersion coefficient

The vertical dispersion coefficient, D_z , results from a combination of molecular diffusion and mechanical dispersion and is defined as (Johnson and Pankow, 1992):

$$D_z = D_e + v_x \alpha_z \quad \text{eq. C.3.23}$$

Where:

- D_e = effective molecular diffusivity (corrected for porosity and tortuosity)
- α_z = vertical dispersivity (typically 0.01 of longitudinal dispersivity)
- v_x = average linear ground-water flow velocity

A typical value of D_e for a nonpolar organic compound is $1 \times 10^{-5} \text{ cm}^2/\text{sec}$ (Sellers and Schreiber, 1992).

“At very low flow velocities where molecular diffusion dominates, the average concentration decreases with increasing flow velocity because of decreasing contact time. At higher groundwater flow velocities where dispersion dominates over diffusion, average percent solubility becomes independent of velocity. This is because the transverse dispersion coefficient is proportional to flow velocity, and D_z/v is constant. At typical groundwater flow velocities, an effluent concentration far less than the solubility limit is expected. For example, for a flow velocity of 1 m/day and $\alpha_z = 10^{-4} \text{ m}$, less than 1 percent of solubility is predicted, and considerable pumping would be required to remove the contaminant. The analysis predicts a constant contaminant concentration dissolved in the extracted water as long as the separate phase covers the boundary” (Hunt *et al.*, 1988, pp. 1253 and 1254).

C.3.3 CONFIRMING AND QUANTIFYING BIODEGRADATION

Chemical evidence of two types can be used to document the occurrence of biodegradation. The first type of evidence is graphical and is provided by the electron acceptor and metabolic byproduct maps discussed in Section C.2. The second line of evidence involves using a conservative tracer.

C.3.3.1 Isopleth Maps

The extent and distribution of contamination relative to electron acceptors and metabolic byproducts can be used to qualitatively document the occurrence of biodegradation. Depleted dissolved oxygen concentrations in areas with fuel hydrocarbon contamination indicates that an active zone of aerobic hydrocarbon biodegradation is present. Depleted nitrate and sulfate concentrations in areas with fuel hydrocarbon contamination indicate that an active zone of anaerobic hydrocarbon biodegradation is present and that denitrification and sulfate reduction are occurring. Elevated iron (II) and methane concentrations in areas with fuel hydrocarbon contamination indicate that an active zone of anaerobic hydrocarbon biodegradation is present and that iron reduction and methanogenesis are occurring. Isopleth maps of contaminants, electron acceptors, and metabolic byproducts can be used as evidence that biodegradation of fuel hydrocarbons is occurring. Figures C.2.7 and C.2.8 show how these maps can be used to support the occurrence of biodegradation. Figure C.2.7 shows that areas with depleted dissolved oxygen, nitrate, and sulfate correspond with areas having elevated BTEX concentrations. Figure C.2.8 shows that areas with elevated iron (II) and elevated methane concentrations also coincide with areas having elevated BTEX concentrations. These figures suggest that aerobic respiration, denitrification, iron reduction, sulfate reduction, and methanogenesis are all occurring at the example site.

C.3.3.2 Data Set Normalization

In order to calculate biodegradation rates accurately, measured contaminant concentrations must be normalized for the effects of dispersion, dilution, and sorption. A convenient way to do this is to use compounds or elements associated with the contaminant plume that are relatively unaffected or predictably affected by biologic processes occurring within the aquifer. At sites where commingled fuel hydrocarbon and chlorinated solvent plumes are present, the trimethylbenzene isomers (TMB), which can be biologically recalcitrant under some geochemical conditions have proven useful when estimating biodegradation rates for BTEX and chlorinated solvents. At sites where TMB data are not available, the chloride produced as a result of biodegradation or the carbon nucleus of the chlorinated compound can be used as a tracer.

Measured concentrations of tracer and contaminant from a minimum of two points along a flow path can be used to estimate the amount of contaminant that would be expected to remain at each point if biodegradation were the only attenuation process operating to reduce contaminant concentrations. The fraction of contaminant remaining as a result of all attenuation processes can be computed from the measured contaminant concentrations at two adjacent points. The fraction of contaminant that would be expected to remain if dilution and dispersion were the only mechanisms for attenuation can be estimated from the tracer concentrations at the same two points. The tracer is affected by dilution and dispersion to the same degree as the contaminant of interest and is not affected by biologic processes. The following equation uses these assumptions to solve for the expected downgradient contaminant concentration if biodegradation had been the only attenuation process operating between two points along the flow path:

$$C_{B,corr} = C_B \left(\frac{T_A}{T_B} \right) \quad \text{eq. C.3.24}$$

Where:

- $C_{B,corr}$ = corrected contaminant concentration at a point B downgradient
 C_B = measured contaminant concentration at point B
 T_A = tracer concentration at a point A upgradient
 T_B = tracer concentration at point B downgradient

This equation can be used to estimate the theoretical contaminant concentration that would result from biodegradation alone for every point along a flow path on the basis of the measured contaminant concentration at the origin and the dilution of the tracer along the flow path. This series of normalized concentrations can then be used to estimate a first-order rate of biodegradation as described in Section C.3.3.3.

C.3.3.2.1 Normalization Using Organic Compounds as Tracers

A convenient way of estimating biodegradation rate constants is to use compounds present in the dissolved contaminant plume that are biologically recalcitrant. One such compound that is useful in some, but not all, ground-water environments is Trimethylbenzene (TMB). The three isomers of this compound (*1,2,3*-TMB, *1,2,4*-TMB, and *1,3,5*-TMB) are generally present in sufficient quantities in fuel mixtures to be readily detectable when dissolved in ground water. When chlorinated solvents enter the subsurface as a mixture with petroleum hydrocarbons, the TMB compounds can be useful tracers. The TMB isomers are fairly recalcitrant to biodegradation under anaerobic conditions; however, the TMB isomers do not make good tracers under aerobic conditions (because they are readily biodegraded in aerobic environments). The degree of recalcitrance of TMB is site-specific, and the use of this compound as a tracer must be evaluated on a case-by-case basis. Nevertheless, if any TMB mass is lost to biodegradation, equation C.3.24 will be conservative because the calculated mass losses and the attenuation rate constants calculated on the basis of those losses will be lower than the actual losses and attenuation rates. Another compound of potential use as a conservative tracer is tetramethylbenzene; however, detectable dissolved tetramethylbenzene concentrations are generally less common than detectable dissolved TMB concentrations.

An ideal tracer would have Henry's Law and soil sorption coefficients identical to the contaminant of interest; however, TMB is more hydrophobic than BTEX, chlorinated ethenes, and chlorinated ethanes, resulting in a higher soil sorption coefficient than the compound of interest. As a result, use of TMB as a tracer is often conservative, and the biodegradation rates can be underestimated. It is best, whenever possible, to compare several tracers to determine whether they are internally consistent.

C.3.3.2.2 Normalization Using Inorganics as Tracers

Inorganic compounds also can serve as tracers for the contaminant of interest as long as their presence is in some way associated (either directly or indirectly) with the dissolved contaminant plume. For many chlorinated solvent plumes, the sum of ionic chloride and organic chloride associated with the solvents can be considered a conservative tracer. Note that the following discussion assumes that the background chloride concentration is negligible in comparison to the source area concentration of total chloride plus chlorine. If background chloride is more than approximately 10 percent of the total source area chloride plus chlorine concentration, then background concentrations will need to be accounted for prior to performing the tracer normalization.

Total chlorine can easily be calculated by multiplying the measured concentration of a chlorinated organic compound by the mass fraction of chlorine in the molecule, then summing that quantity for all the chlorinated organic compounds represented in the plume. The stoichiometry for chlorinated ethenes is presented in the following paragraphs.

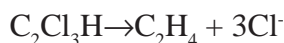
As PCE is reduced to ethene, 4 moles of chloride are produced:



On a mass basis, the ratio of chloride produced to PCE degraded is given by:

Molecular weights:	PCE	$2(12.011) + 4(35.453) = 165.83 \text{ gm}$
	Chloride	$4(35.453) = 141.81 \text{ gm}$
Mass Ratio of Chloride to PCE = $141.81:165.83 = 0.86:1$		

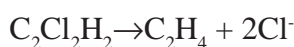
Similarly, as TCE is reduced to ethene, 3 moles of chloride are produced:



On a mass basis, the ratio of chloride produced to TCE degraded is given by:

Molecular weights:	TCE	$2(12.011) + 3(35.453) + 1(1.01) = 131.39 \text{ gm}$
	Chloride	$3(35.453) = 106.36 \text{ gm}$
Mass Ratio of Chloride to TCE = $106.36:131.39 = 0.81:1$		

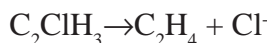
Likewise, as DCE is reduced to ethene, 2 moles of chloride are produced:



On a mass basis, the ratio of chloride produced to DCE degraded is given by:

Molecular weights:	DCE	$2(12.011) + 2(35.453) + 2(1.01) = 96.95 \text{ gm}$
	Chloride	$2(35.453) = 70.9 \text{ gm}$
Mass Ratio of Chloride to DCE = $70.9:96.95 = 0.73:1$		

As VC is reduced to ethene, 1 mole of chloride is produced:



On a mass basis, the ratio of chloride produced to VC degraded is given by:

Molecular weights:	VC	$2(12.011) + 1(35.453) + 3(1.01) = 62.51 \text{ gm}$
	Chloride	$1(35.453) = 35.453 \text{ gm}$
Mass Ratio of Chloride to VC = $35.453:62.51 = 0.57:1$		

Therefore, the amount of total chloride plus chlorine for a spill undergoing reductive dechlorination would be estimated as:

$$[\text{Cl}_{\text{Total}}] = 0.86[\text{PCE}] + 0.81[\text{TCE}] + 0.73[\text{DCE}] + 0.57[\text{VC}] \quad \text{eq. C.3.25}$$

Example C.3.4: Calculating Total Concentration of Chloride and Organic Chlorine

The approach is illustrated in the following data set from the West TCE Plume at the St. Joseph, Michigan NPL site.

A series of discrete vertical water samples were taken in transects that extended across the plume at locations downgradient of the source of TCE. The locations of the samples are depicted in Figure C.3.5 as circles. At each sampling location, water samples were acquired using a hollow-stem auger. The leading auger was slotted over a five-foot interval. After a sample was collected, the auger was driven five feet further into the aquifer and the next sample was collected. At any one location, the water samples were collected in a sequential and continuous series that extended from the water table to a clay layer at the bottom of the aquifer. The concentrations of contaminants at each location were averaged in water samples that extend across the entire vertical extent of the plume. The location with the highest average concentration of chlorinated ethenes in a particular transect was selected to represent the centerline of the plume. The locations of the sample locations in the centerline of the plume are depicted in Figure C.3.5 as open circles. Each centerline location is labelled in an oval.

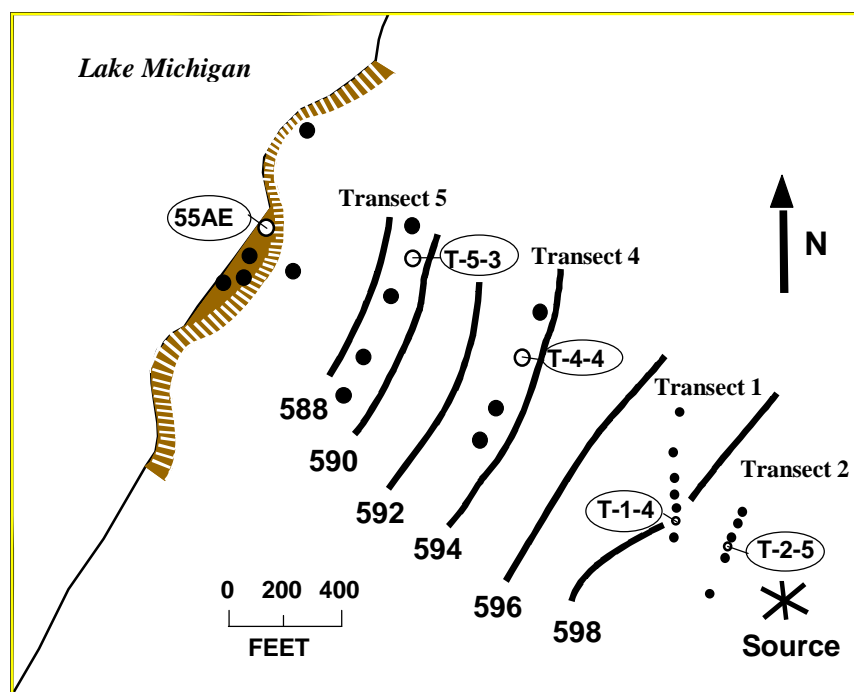


Figure C.3.4 Location of sampling points at the St. Joseph, Michigan, NPL site.

The concentrations of chlorinated ethenes and chloride in the centerline of the TCE plume at St. Joseph, Michigan, are presented in Table C.3.5.

Table C.3.5 Attenuation of Chlorinated Ethenes and Chloride Downgradient of the Source of TCE in the West Plume at the St. Joseph, Michigan, NPL Site.

Compound	Sampling Locations				
	T-2-5	T-1-4	T-4-2	T-5-3	55AE
	Distance Downgradient (feet)				
	0	200	1,000	1,500	2,000
	----- (mg/Liter) -----				
PCE	0.0	0.0	0.0	0.0	0.0
TCE	12.1	3.4	1.3	0.035	0.022
Total DCE	37.6	11.7	2.4	0.23	0.45
Vinyl Chloride	2.3	3.7	0.51	0.063	0.070
Total Organic Chloride	38.5	13.4	3.2	0.2	0.4
Chloride	89.7	78.6	98.9	63.6	54.7
Tracer (Total Chloride plus Chlorine)	128.2	92.0	102.1	63.8	55.1

At the monitoring point closest to the source of the plume (see location T-2-5 in Table C.3.5 and Figure C.3.4) the concentrations of TCE, total DCE, vinyl chloride and chloride were 12.1, 37.6, 2.3 and 89.7 mg/L, respectively. This results in an upgradient tracer concentration of

TCE chlorine	+	(0.809)(12.1 mg/L)
DCE chlorine	+	(0.731)(37.6 mg/L)
Vinyl chloride chlorine	+	(0.567)(2.3 mg/L)
Chloride	+	89.7 mg/L
Total chloride plus chlorine	=	128.2 mg/L

At the downgradient location 55AE, which is 2,000 feet from the source, the concentrations of TCE, total DCE, vinyl chloride, and chloride were 0.022, 0.45, 0.070, and 54.70 mg/L, respectively. This results in a downgradient concentration of

TCE chlorine	+	(0.809)(0.022 mg/L)
DCE chlorine	+	(0.731)(0.45 mg/L)
Vinyl chloride chlorine	+	(0.567)(0.070 mg/L)
Chloride	+	54.7 mg/L
Total chloride plus chlorine	=	55.1 mg/L

The computed series of total chloride plus chlorine concentrations can be used with equation C.3.24 to estimate a normalized data set for contaminant concentrations.

Example C.3.5: Normalizing Contaminant Concentrations Along a Flow Path

Equation 3.24 will be used to calculate a normalized concentration for TCE at the locations depicted in Figure C.3.4 and Table C.3.5. Given are the observed concentrations of TCE and tracer (Table C.3.5) for five points that form a line parallel to the direction of ground-water flow (Figure C.3.4) To calculate normalized concentrations of TCE using the attenuation of the tracer, the dilution of the tracer is calculated at each location by dividing the concentration of tracer at the source (or most contaminated location) by the concentration of tracer at each downgradient location. Then the measured concentration of TCE downgradient is multiplied by the dilution of the tracer. The corrected concentrations of TCE are presented in Table C.3.6. This information will be used in sections C.3.3.3 to calculate the rate of natural biodegradation of TCE.

Table C.3.6. *Use of the Attenuation of a Tracer to Correct the Concentration of TCE Downgradient of the Source of TCE in the West Plume at the St. Joseph, Michigan, NPL Site*

Compound	Sampling Locations				
	T-2-5	T-1-4	T-4-2	T-5-3	55AE
	Distance Down Gradient (feet)				
	0	200	1,000	1,500	2,000
	----- (mg/Liter) -----				
TCE	12.1	3.4	1.3	0.035	0.022
Tracer	128.2	92.0	102.1	63.8	55.1
Dilution of Tracer	128.2/ 28.2	128.2/ 92.0	128.2/ 102.1	128.2/ 63.8	128.2/ 55.1
Corrected TCE	12.1	4.7	1.6	0.070	0.051

C.3.3.3 Calculating Biodegradation Rates

Several methods, including first- and second-order approximations, may be used to estimate the rate of biodegradation of chlorinated compounds when they are being used to oxidize other organic compounds. Use of the first-order approximation can be appropriate to estimate biodegradation rates

for chlorinated compounds when the rate of biodegradation is controlled solely by the concentration of the contaminant. However, the use of a first-order approximation may not be appropriate when more than one substrate is limiting microbial degradation rates or when microbial mass is increasing or decreasing. In such cases, a second- or higher-order approximation may provide a better estimate of biodegradation rates.

C.3.3.3.1 First-Order Decay

As with a large number of processes, the change in a solute's concentration in ground water over time often can be described using a first-order rate constant. A first-order approximation, if appropriate, has the advantage of being easy to calculate and simplifies fate and transport modeling of complex phenomenon. In one dimension, first-order decay is described by the following ordinary differential equation:

$$\frac{dC}{dt} = -kt \quad \text{eq. C.3.26}$$

Where:

C = concentration at time t [M/L³]

k = overall attenuation rate (first-order rate constant) [1/T]

Solving this differential equation yields:

$$C = C_o e^{-kt} \quad \text{eq. C.3.27}$$

The overall attenuation rate groups all processes acting to reduce contaminant concentrations and includes advection, dispersion, dilution from recharge, sorption, and biodegradation. To determine the portion of the overall attenuation that can be attributed to biodegradation, these effects must be accounted for, and subtracted from the total attenuation rate.

Aronson and Howard (1997) have compiled a large number of attenuation rate constants for biodegradation of organic compounds in aquifers. This information is supplied to provide a basis for comparison of rate constants determined for at a particular site to the general experience with natural attenuation as documented in the literature. It is not intended to provide rate constants for a site in a risk assessment or exposure assessment. The rate constants used to describe behavior of a particular site must be extracted from site characterization information particular to that site.

The distribution of the rate constants reported for TCE is presented in Figure C.3.5. Notice that the average rate is near 1.0 per year, and that most of the rates cluster in a relatively narrow range between 3.0 per year and 0.3 per year. Some of the published rates are very low, less than 0.1 per year. The report compiles data from sites where rates are published. The general bias against publishing negative data suggests that there are many plumes where TCE attenuation was not detectable (Type 3 behavior), and that data on these plumes is not found in the literature. The data from Aronson and Howard (1997) reflect the behavior of plumes where reductive dechlorination is an important mechanism (Type 1 and Type 2 sites). Rate constants for PCE and Vinyl Chloride are presented in Figures C.3.6 and C.3.7. The average rate for dechlorination of PCE is somewhat faster than for TCE, near 4.0 per year, and the rate for Vinyl Chloride is slower, near 0.6 per year.

Two methods for determining first-order biodegradation rates at the field scale are presented. The first method involves the use of a normalized data set to compute a decay rate. The second method was derived by Buscheck and Alcantar (1995) and is valid for steady-state plumes. Wiedemeier *et al.* (1996b) compare the use of these two methods with respect to BTEX biodegradation.

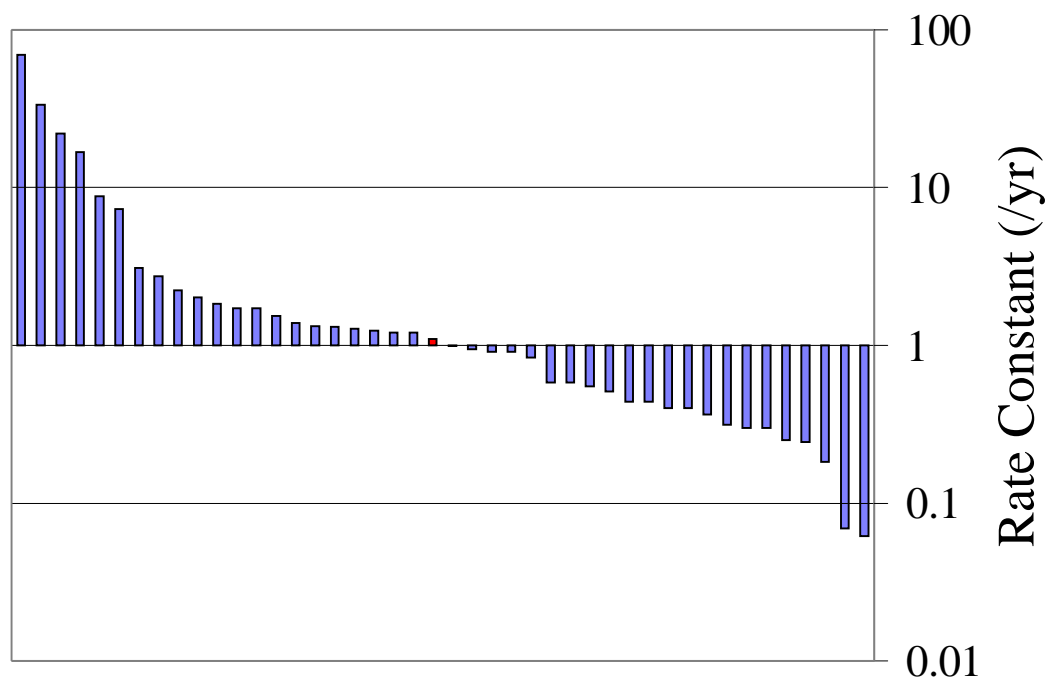


Figure C.3.5. Field rate constants for TCE as reported in literature.

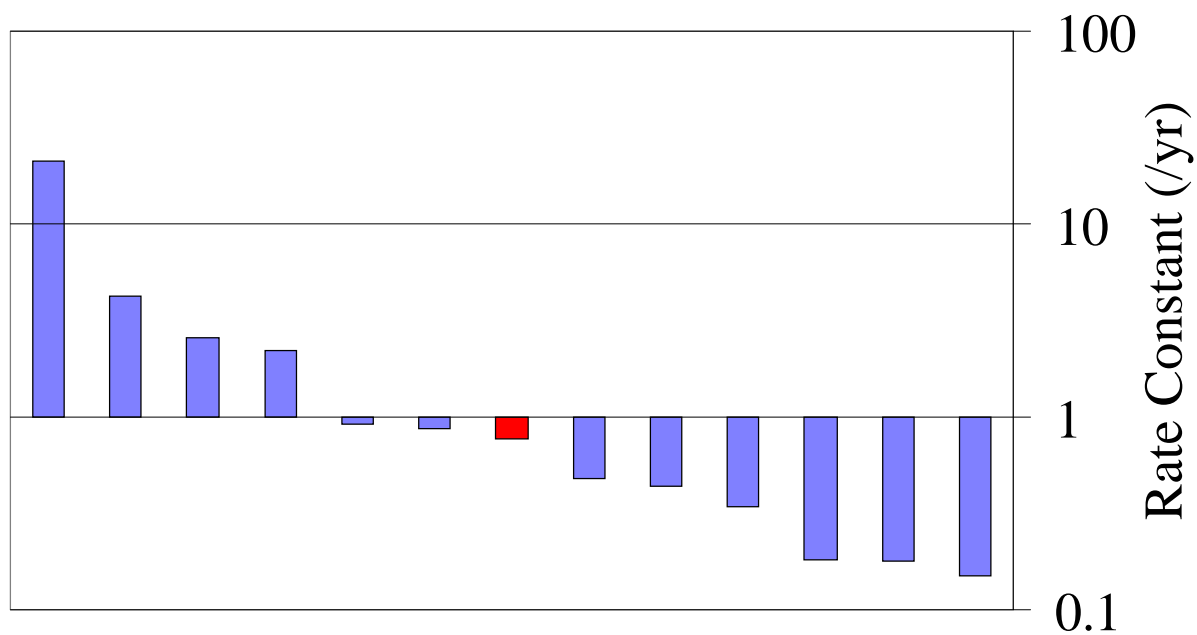


Figure C.3.6 Field rate constants for PCE as reported in literature.

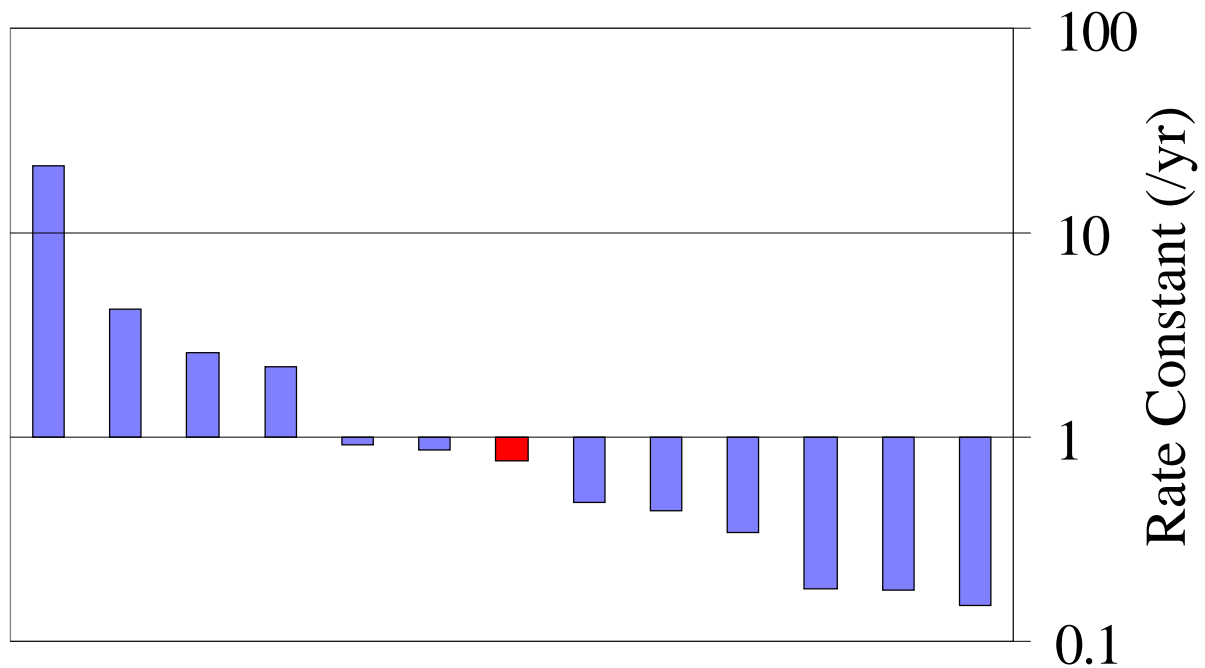


Figure C.3.7 Field rate constants for vinyl chloride as reported in literature.

C.3.3.3.2 Use of a Normalized Data Set

In order to ensure that observed decreases in contaminant concentrations can be attributed to biodegradation, measured contaminant concentrations must be corrected for the effects of advection, dispersion, dilution from recharge, and sorption, as described in Section C.3.3.2 using equation C.3.24. The corrected concentration of a compound is the concentration that would be expected at one point (B) located downgradient from another point (A) if the processes of dispersion and dilution had not been occurring between points A and B.

The biodegradation rate can be estimated between any two points (A and B) of a normalized data set (where point A is upgradient of point B) by substituting the concentration at point A for C_0 , and the normalized concentration at point B, $C_{B,corr}$, for C in equation C.3.27. The resulting relationship is expressed as:

$$C_{B,corr} = C_A e^{-\lambda t} \quad \text{eq. C.3.28}$$

Where:

- $C_{B,corr}$ = normalized contaminant concentration at downgradient point B (from eq. C.3.25)
- C_A = contaminant concentration at upgradient point A that if point A is the first point in the normalized data set, then $C_A = C_{A,corr}$
- λ = first-order biological decay rate (first-order rate constant) [1/T]
- t = time of contaminant travel between points A and B

The rate constant in this equation is no longer the total attenuation rate, k , but is the biological decay rate, λ , because the effects of advection, dispersion, dilution from recharge, and sorption have been removed (Section C.3.3.2). This relationship can be used to calculate the first-order biological decay rate constant between two points by solving equation C.3.28 for λ :

$$\lambda = -\frac{\ln\left(\frac{C_{B,corr}}{C_A}\right)}{t} \quad \text{eq. C.3.29}$$

The travel time, t , between two points is given by:

$$t = \frac{x}{v_c} \quad \text{eq. C.3.30}$$

Where:

x = distance between two points [L]

v_c = retarded solute velocity [L/T]

Example C.3.6: First-Order Decay Rate Constant Calculation Using Normalized Data Set

Equation C.3.30 and C.3.29 can be used to calculate rate constants between any two points along a flow line. For travel from locations T-2-5 and 55AE in Figure C.3.4 and Table C.3.6, the upgradient concentration of TCE is 12.1 mg/l, the corrected downgradient concentration is 0.051 mg/l, and the distance between the locations is 2,000 feet.

From Figure C.3.4, the water table drops 10 feet as the plume moves 1,300 feet from transect 1 to transect 5. The site has a hydraulic gradient of 0.008 feet per foot. Aquifer testing at the site predicts an average hydraulic conductivity of 50 feet per day. If the effective porosity of the sandy aquifer is assumed to be 0.3, the seepage velocity (V_x) would be (Equation C.3.6):

$$V_x = \frac{0.4 \text{ ft/day} \times 0.008 \text{ ft/ft}}{0.3} = 1.3 \text{ ft/day}$$

The average organic matter content of the aquifer matrix material is less than the detection limit of 0.001 g/g. We will assume the organic matter content is equal to the detection limit. If the K_{oc} of TCE is 120 ml/g, the porosity is 0.3, and the bulk density is 1.7 gm/cm³, the distribution of TCE between ground water and aquifer solids is the product of the K_{oc} , the fraction organic carbon, the bulk density, divided by the porosity, or 0.3. The retarded velocity of TCE compared to water (R) would be (Equation C.3.8 and Equation C.3.13):

$$R = 1 + 120 \text{ (ml/g)} * 0.001 \text{ (g/g)} * 1.7 \text{ (g/cm}^3\text{)} / 0.3 \text{ (ml/ml)} = 1.7$$

The velocity of TCE in the aquifer would be equal to the velocity of water in the plume divided by the retardation of TCE. The TCE velocity (v_c) would be:

$$v_c = 1.3 \text{ feet per day} / 1.7 = 0.8 \text{ feet per day}$$

If the distance between the wells is 2,000 feet, and the retarded velocity of TCE is 0.8 feet per day, by equation C.3.30 the travel time is:

$$t = 2,000 \text{ feet} / 0.8 \text{ feet per day} = 2,500 \text{ days} = 6.8 \text{ years}$$

From equation C.3.29, the rate of biotransformation between locations T-2-5 and 55AE is:

$$\lambda = \ln(0.055/12.1) / 6.8 \text{ per year} = 0.79 \text{ per year}$$

If a number of sampling locations are available along a flow path, all the locations should be included in the calculation of the biotransformation rate. The simplest way to determine the first-order rate constant from an entire set of normalized data is to make a log-linear plot of normalized contaminant concentrations versus travel time. If the data plot along a straight line, the relationship is first-order and an exponential regression analysis can be performed.

The exponential regression analysis gives the equation of the line of best fit for the data being regressed from a log-linear plot and has the general form:

$$y = be^{mx}$$

eq. C.3.31

Where:

- y = y axis value
- b = y intercept
- m = slope of regression line
- x = x-axis value

When using normalized data, x is the contaminant travel time to the downgradient locations and m is the first-order rate of change equal to the negative. The correlation coefficient, R^2 , is a measure of how well the regression relationship approximates the data. Values of R^2 can range from 0 to 1; the closer R^2 is to 1, the more accurate the equation describing the trend in the data. Values of R^2 greater than 0.80 are generally considered useful; R^2 values greater than 0.90 are considered excellent. Several commonly available spreadsheets can be used to facilitate the exponential regression analysis. The following example illustrates the use of this technique.

Figure C.3.8 depicts a regression of normalized TCE concentration against travel time downgradient. The slope of the exponential regression is $-0.824x$ where x is travel time in years, corresponding to a first-order rate of change of -0.824 per year and a first-order rate of biodegradation of 0.824 per year. In Figure C.3.8, an exponential regression was performed on the normalized concentrations of TCE against time of travel along the flow path. An alternative approach would be to perform a linear regression of the natural logarithm of the normalized concentration of TCE against travel time along the flow path.

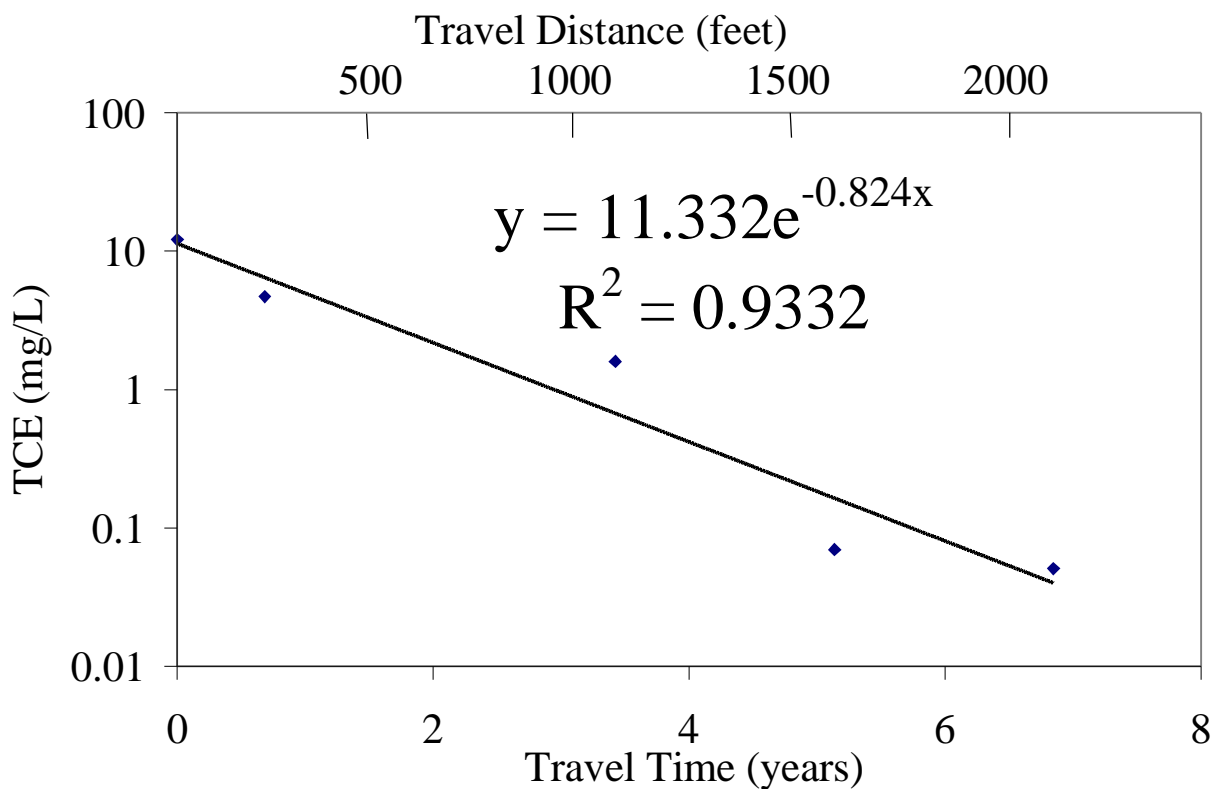


Figure C.3.8 Exponential regression of TCE concentration on time of travel along flow path.

C.3.3.3.3. Method of Buscheck and Alcantar (1995)

Buscheck and Alcantar (1995) derive a relationship that allows calculation of first-order decay rate constants for steady-state plumes. This method involves coupling the regression of contaminant concentration (plotted on a logarithmic scale) versus distance downgradient (plotted on a linear scale) to an analytical solution for one-dimensional, steady-state, contaminant transport that includes advection, dispersion, sorption, and biodegradation. For a steady-state plume, the first-order decay rate is given by (Buscheck and Alcantar, 1995):

$$\lambda = \frac{v_c}{4\alpha_x} \left(\left[1 + 2\alpha_x \left(\frac{k}{v_x} \right) \right]^2 - 1 \right) \quad \text{eq. C.3.32}$$

Where:

λ = first-order biological rate constant

v_c = retarded contaminant velocity in the x-direction

α_x = dispersivity

k/v_x = slope of line formed by making a ln-linear plot of contaminant concentration versus distance downgradient along flow path

Example C.3.7: First-Order Rate Constant Calculation Using Method of Buscheck and Alcantar (1995)

The first step is to confirm that the contaminant plume has reached a steady-state configuration. This is done by analyzing historical data to make sure that the plume is no longer migrating downgradient and that contaminant concentrations are not changing significantly through time. This is generally the case for older spills where the source has not been removed. The next step is to make a plot of the natural logarithm of contaminant concentration versus distance downgradient (see Figure C.3.9). Using linear regression, y in the regression analysis is the contaminant concentration, x is the distance downgradient from the source, and the slope of the ln-linear regression is the ratio k/v_x that is entered into equation C.3.32.

The slope is -0.0028 feet. As calculated above, the retarded TCE velocity in the plume v_c is 0.8 feet per day. If $\alpha_x = 5\%$ of the plume length, then $\alpha_x = 100$ feet. Inserting these values for α_x , k/v_x , and v_c into equation C.3.32, the estimated value of $\lambda = -0.0016$ per day or -0.59 per year.

C.3.3.2.2.3 *Comparison of First-Order Methods*

If the data are available, concentrations of tracers should be used to normalize concentrations of contaminants prior to calculation of rate constants. If tracer data is not available, the method of Buscheck and Alcantar (1995) can be used if a value for longitudinal dispersion is available, or if one is willing to assume a value for longitudinal dispersion. Whenever possible, more than one tracer should be used to normalize the concentrations of contaminants. If the normalized concentrations agree using several different tracers, the approach can be accepted with confidence. In addition to chloride and trimethylbenzene, methane, and total organic carbon dissolved in ground water are often useful tracers in plumes of chlorinated solvents undergoing natural attenuation.

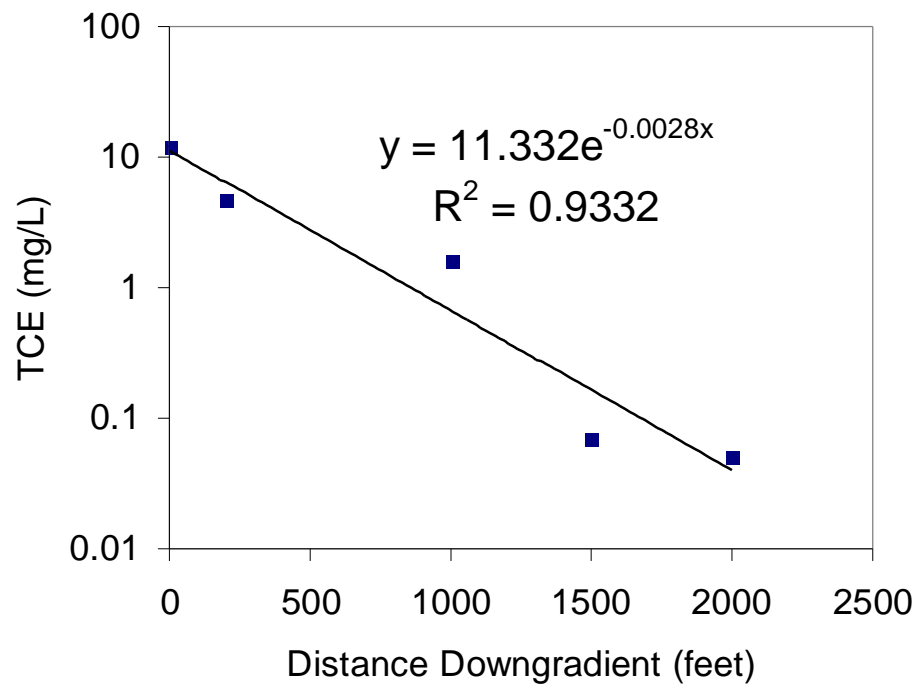


Figure C.3.9 Regression of the TCE concentration on distance along flow path.

C.3.4 DESIGN, IMPLEMENTATION, AND INTERPRETATION OF MICROCOSM STUDIES

C.3.4.1 Overview

If properly designed, implemented, and interpreted, microcosm studies can provide very convincing documentation of the occurrence of intrinsic bioremediation. They are the only “line of evidence” that allows an unequivocal mass balance on the biodegradation of environmental contaminants. If the microcosm study is properly designed, it will be easy for decision makers with non-technical backgrounds to interpret. The results of a microcosm study are strongly influenced by the nature of the geological material submitted to study, by the physical properties of the microcosm, by the sampling strategy, and the duration of the study. In addition, microcosm studies are time consuming and expensive. A microcosm study should only be undertaken at sites where there is considerable uncertainty concerning the biodegradation of contaminants based on soil and ground-water samples alone.

Material for a microcosm study should not be selected until the geochemical behavior of the site is well understood. Contaminant plumes may consume oxygen, nitrate, or sulfate, and produce iron (II), manganese (II), or methane. These processes usually operate concurrently in different parts of the plume. Regions where each process prevails may be separated in directions parallel to ground-water flow by hundreds of meters, in directions perpendicular to ground-water flow by tens of meters, and vertically by only a few meters. Rate constants and constraints for petroleum hydrocarbon biodegradation will be influenced by the prevailing geochemistry. Material from microcosms must be acquired for depth intervals and locations that have been predetermined to be representative of the prevailing geochemical milieu in the plume.

Contaminant biodegradation supported by oxygen and nitrate cannot be adequately represented in microcosm. In the field, organisms that use oxygen or nitrate proliferate until they become limited by the supply of electron acceptor. After that time, the rate of hydrocarbon degradation is controlled by the supply of electron acceptor through diffusion or hydrodynamic dispersion. Microcosms have been used successfully to simulate sulfate-reducing, iron-reducing, and methanogenic regions of plumes. Oxygen is toxic to sulfate-reducing and methanogenic microorganisms. Material should be collected and secured in a manner that precludes oxygenation of the sample.

Batch microcosms that are sacrificed for each analysis usually give more interpretable results than column microcosms or batch microcosms that are sampled repetitively. For statistical reasons, at least three microcosms should be sampled at each time interval. If one assumes a first-order rate law, and no lag, a geometrical time interval for sampling should be the most efficient. An example would be sampling after 0 weeks, 2 weeks, 1 month, 2 months, 4 months, and 8 months. As a practical matter, long lags frequently occur, and the rate of bioremediation after the lag is rapid. A simple linear time scale is most likely to give interpretable results.

The batch microcosms should have approximately the same ratio of solids to water as the original material. Most of the microbes are attached to solids. If a microcosm has an excess of water, and the contaminant is mostly in the aqueous phase, the microbes must process a great deal more contaminant to produce the same relative change in the contaminant concentration as would be obtained at field scale. The kinetics at field scale would be underestimated.

Microcosms are inherently time consuming. At field scale, the residence time of a plume may be several years to decades. Slow rates of transformation may have a considerable environmental significance. A microcosm study that lasts only a few weeks or months may not have the resolution to detect slow changes that are still of environmental significance. Further, microcosms often show a pattern of sequential utilization, with toluene and the xylenes degrading first, and benzene and ethylbenzene degrading at a later time. Degradation of benzene or ethylbenzene may be delayed by as much as a year.

As a practical matter, batch microcosms with an optimal solids-to-water ratio, sampled every 2 months in triplicate for up to 18 months, can resolve biodegradation from abiotic losses with a rate detection limit of 0.001 to 0.0005 per day. Many plumes show significant attenuation of contamination at field-calibrated rates that are slower than the detection limit of today's microcosm technology. The most appropriate use of microcosms is to document that contaminant attenuation is largely a biological process. Rate constants for modeling purposes are more appropriately acquired from field-scale studies.

Microcosm studies are often used to provide a third line of evidence. The potential for biodegradation of the contaminants of interest can be confirmed by the use of microcosms, through comparison of removals in the living treatments with removals in the controls. Microcosm studies also permit an absolute mass balance determination based on biodegradation of the contaminants of interest. Further, the appearance of daughter products in the microcosms can be used to confirm biodegradation of the parent compound.

C.3.4.2 When to Use Microcosms

There are two fundamentally different applications of microcosms. They are frequently used in a qualitative way to illustrate the important processes that control the fate of organic contaminants. They are also used to estimate rate constants for biotransformation of contaminants that can be used in a site-specific transport and fate model of a plume of contaminated groundwater. This paper only discusses microcosms for the second application.

Microcosms should be used when there is no other way to obtain a rate constant for attenuation of contaminants, in particular, when it is impossible to estimate the rate of attenuation from data from monitoring wells in the plume of concern. There are situations where it is impossible to compare concentrations in monitoring wells along a flow path due to legal or physical impediments. In many landscapes, the direction of ground-water flow (and water table elevations in monitoring wells) can vary over short periods of time due to tidal influences or changes in barometric pressure. The direction of ground-water flow may also be affected by changes in the stage of a nearby river or pumping wells in the vicinity. These changes in ground-water flow direction do not allow simple snap-shot comparisons of concentrations in monitoring wells because of uncertainties in identifying the flow path. Rate constants from microcosms can be used with average flow conditions to estimate attenuation at some point of discharge or point of compliance.

C.3.4.3 Application of Microcosms

The primary objective of microcosm studies is to obtain rate constants applicable to average flow conditions. These average conditions can be determined by continuous monitoring of water table elevations in the aquifer being evaluated. The product of the microcosm study and the continuous monitoring of water table elevations will be a yearly or seasonal estimate of the extent of attenuation along average flow paths. Removals seen at field scale can be attributed to biological activity. If removals in the microcosms duplicate removal at field scale, the rate constant can be used for risk assessment purposes (B.H. Wilson *et al.*, 1996; Bradley, *et al.*, 1998).

C.3.4.4 Selecting Material for Study

Prior to choosing material for microcosm studies, the location of major conduits of ground-water flow should be identified and the geochemical regions along the flow path should be determined. The important geochemical regions for natural attenuation of chlorinated aliphatic hydrocarbons are regions that are actively methanogenic; regions that exhibit sulfate reduction and iron reduction concomitantly; and regions that exhibit iron reduction alone. The pattern of biodegradation of chlorinated solvents varies in different regions. Vinyl chloride tends to accumulate during reductive dechlorination of TCE or PCE in methanogenic regions (Weaver *et al.*, 1995; J.T. Wilson *et al.*, 1995); it does not accumulate to the same extent in regions exhibiting iron reduction and

sulfate reduction (Chapelle, 1996). In regions showing iron reduction alone, vinyl chloride is consumed but dechlorination of PCE, TCE, or DCE may not occur (Bradley and Chapelle, 1996;1997). Core material from each geochemical region in major flow paths represented by the plume must be acquired, and the hydraulic conductivity of each depth at which core material is acquired must be measured. If possible, the microcosms should be constructed with the most transmissive material in the flow path.

Several characteristics of ground water from the same interval used to collect the core material should be determined. These characteristics include temperature, redox potential, pH, and concentrations of oxygen, sulfate, sulfide, nitrate, iron II, chloride, methane, ethane, ethene, total organic carbon, and alkalinity. The concentrations of compounds of regulatory concern and any breakdown products for each site must be determined. The ground water should be analyzed for methane to determine if methanogenic conditions exist and for ethane and ethene as daughter products from reductive dechlorination of PCE and TCE. A comparison of the ground-water chemistry from the interval where the cores were acquired to that in neighboring monitoring wells will demonstrate if the collected cores are representative of that section of the contaminant plume.

Reductive dechlorination of chlorinated solvents requires an electron donor to allow the process to proceed. The electron donor could be soil organic matter, low molecular weight organic compounds (lactate, acetate, methanol, glucose, etc.), H_2 , or a co-contaminant such as landfill leachate or petroleum compounds (Bouwer, 1994; Sewell and Gibson, 1991; Klecka *et al.*, 1996). In many instances, the actual electron donor(s) may not be identified.

Several characteristics of the core material should also be evaluated. The initial concentration of the contaminated material (on a mass per mass basis) should be identified prior to construction of the microcosms. Also, it is necessary to know if the contamination is present as a nonaqueous phase liquid (NAPL) or in solution. A total petroleum hydrocarbon (TPH) analysis will determine if any hydrocarbon-based oily materials are present. The water-filled porosity is a parameter generally used to extrapolate rates to the field. It can be calculated by comparing wet and dry weights of the aquifer material.

To insure sample integrity and stability during acquisition, it is important to quickly transfer the aquifer material into a jar, exclude air by adding ground water, and seal the jar without headspace. The material should be cooled during transportation to the laboratory. Incubate the core material at the ambient ground-water temperature in the dark before the construction of microcosms.

At least one microcosm study per geochemical region should be completed. If the plume is over one kilometer in length, several microcosm studies per geochemical region may need to be constructed.

C.3.4.5 Geochemical Characterization of the Site

The geochemistry of the subsurface affects behavior of organic and inorganic contaminants, inorganic minerals, and microbial populations. Major geochemical parameters that characterize the subsurface encompasses (1) pH; (2) ORP; (3) alkalinity; (4) physical and chemical characterization of the solids; (5) temperature; (6) dissolved constituents, including electron acceptors; and (7) microbial processes. The most important of these in relation to biological processes are redox potential, alkalinity, concentration of electron acceptor, and chemical nature of the solids.

Alkalinity: Field indications of biologically active portions of a plume may be identified by increased alkalinity, compared to background wells, from carbon dioxide due to biodegradation of the pollutants. Increases in both alkalinity and decrease in pH have been measured in portions of an aquifer contaminated by gasoline undergoing active utilization of the gasoline components (Cozzarelli *et al.*, 1995). Alkalinity can be one of the parameters used when identifying where to collect biologically active core material.

pH: Bacteria generally prefer a neutral or slightly alkaline pH level with an optimum pH range for most microorganisms between 6.0 and 8.0; however, many microorganisms can tolerate a pH range of 5.0 to 9.0. Most ground waters in uncontaminated aquifers are within these ranges. Natural pH values may be as low as 4.0 or 5.0 in aquifers with active oxidation of sulfides, and pH values as high as 9.0 may be found in carbonate-buffered systems (Chapelle, 1993). However, pH values as low as 3.0 have been measured for ground waters contaminated with municipal waste leachates which often contain elevated concentrations of organic acids (Baedecker and Back, 1979). In ground waters contaminated with sludges from cement manufacturing, pH values as high as 11.0 have been measured (Chapelle, 1993).

ORP: The ORP of ground water is a measure of electron activity that indicates the relative ability of a solution to accept or transfer electrons. Most redox reactions in the subsurface are microbially catalyzed during metabolism of native organic matter or contaminants. The only elements that are predominant participants in aquatic redox processes are carbon, nitrogen, oxygen, sulfur, iron, and manganese (Stumm and Morgan, 1981). The principal oxidizing agents in ground water are oxygen, nitrate, sulfate, manganese (IV), and iron (III). Biological reactions in the subsurface both influence and are affected by the redox potential and the available electron acceptors. The redox potential changes with the predominant electron acceptor, with reducing conditions increasing through the sequence oxygen, nitrate, iron, sulfate, and carbonate. The redox potential decreases in each sequence, with methanogenic (carbonate as the electron acceptor) conditions being most reducing. The interpretation of redox potentials in ground waters is difficult (Snoeyink and Jenkins, 1980). The potential obtained in ground waters is a mixed potential that reflects the potential of many reactions and cannot be used for quantitative interpretation (Stumm and Morgan, 1981). The approximate location of the contaminant plume can be identified in the field by measurement of the redox potential of the ground water.

To overcome the limitations imposed by traditional redox measurements, recent work has focused on the measurement of molecular hydrogen to accurately describe the predominant *in situ* redox reactions (Chapelle *et al.*, 1995; Lovley *et al.*, 1994; Lovley and Goodwin, 1988). The evidence suggests that concentrations of H₂ in ground water can be correlated with specific microbial processes, and these concentrations can be used to identify zones of methanogenesis, sulfate reduction, and iron reduction in the subsurface (Chapelle, 1996).

Electron Acceptors: Measurement of the available electron acceptors is critical in identifying the predominant microbial and geochemical processes occurring *in situ* at the time of sample collection. Nitrate and sulfate are found naturally in most ground waters and will subsequently be used as electron acceptors once oxygen is consumed. Oxidized forms of iron and manganese can be used as electron acceptors before sulfate reduction commences. Iron and manganese minerals solubilize coincidentally with sulfate reduction, and their reduced forms scavenge oxygen to the extent that strict anaerobes (some sulfate reducers and all methanogens) can develop. Sulfate is found in many depositional environments, and sulfate reduction may be very common in many contaminated ground waters. In environments where sulfate is depleted, carbonate becomes the electron acceptor with methane gas produced as an end product.

Temperature: The temperature at all monitoring wells should be measured to determine when the pumped water has stabilized and is ready for collection. Below approximately 30 feet, the temperature in the subsurface is fairly consistent on an annual basis. Microcosms should be stored at the average *in situ* temperature. Biological growth can occur over a wide range of temperatures, although most microorganisms are active primarily between 10°C and 35°C (50°F to 95°F).

Chloride: Reductive dechlorination results in the accumulation of inorganic chloride. In aquifers with a low background of inorganic chloride, the concentration of inorganic chloride should

increase as the chlorinated solvents are degraded. The sum of the inorganic chloride plus the chloride in the contaminant being degraded should remain relatively consistent along the ground water flow path.

Tables C.3.7 and C.3.8 list the geochemical parameters, contaminants, and daughter products that should be measured during site characterization for natural attenuation. The tables include the analyses that should be performed, the optimum range for natural attenuation of chlorinated solvents, and the interpretation of the value in relation to biological processes.

Table C.3.7 *Geochemical Parameters Important to Microcosm Studies*

Analysis	Range	Interpretation
Redox Potential	<50 millivolt against Ag/AgCl	Reductive pathway possible
Sulfate	<20 mg/L	Competes at higher concentrations with reductive pathway
Nitrate	<1 mg/L	Competes at higher concentrations with reductive pathway
Oxygen	<0.5 mg/L	Tolerated, toxic to reductive pathway at higher concentrations
Oxygen	>1 mg/L	Vinyl chloride oxidized
Iron (II)	>1 mg/L	Reductive pathway possible
Sulfide	>1 mg/L	Reductive pathway possible
Hydrogen	>1 nM	Reductive pathway possible, vinyl chloride may accumulate
Hydrogen	<1 nM	Vinyl chloride oxidized
pH	5 < pH < 9	Tolerated range

Table C.3.8 *Contaminants and Daughter Products Important to Microcosm Studies*

Analysis	Interpretation
PCE	Material spilled
TCE	Material spilled or daughter product of PCE
1,1,1-TCA	Material spilled
<i>cis</i> -1,2-DCE	Daughter product of TCE
<i>trans</i> -1,2-DCE	Daughter product of TCE
Vinyl Chloride	Daughter product of dichloroethylenes
Ethene	Daughter product of vinyl chloride
Ethane	Daughter product of ethene
Methane	Ultimate reductive daughter product
Chloride	Daughter product of organic chlorine
Carbon Dioxide	Ultimate oxidative daughter product
Alkalinity	Results from interaction of carbon dioxide with aquifer minerals

C.3.4.6 Microcosm Construction

During construction of the microcosms, it is best if all manipulations take place in an anaerobic glovebox. These gloveboxes exclude oxygen and provide an environment where the integrity of the core material may be maintained, since many strict anaerobic bacteria are sensitive to oxygen. Stringent aseptic precautions not necessary for microcosm construction. It is more important to maintain anaerobic conditions of the aquifer material and solutions added to the microcosm bottles.

The microcosms should have approximately the same ratio of solids to water as the *in situ* aquifer material, with a minimum or negligible headspace. Most bacteria in the subsurface are attached to the aquifer solids. If a microcosm has an excess of water, and the contaminant is primarily in the dissolved phase, the bacteria must consume or transform a great deal more contaminant to produce the same relative change in the contaminant concentration. As a result, the kinetics of removal at field scale will be underestimated in the microcosms.

A minimum of three replicate microcosms for both living and control treatments should be constructed for each sampling event. Microcosms sacrificed at each sampling interval are preferable to microcosms that are repetitively sampled. The compounds of regulatory interest should be added at concentrations representative of the higher concentrations found in the geochemical region of the plume being evaluated. The compounds should be added as a concentrated aqueous solution. If an aqueous solution is not feasible, dioxane or acetonitrile may be used as solvents. Avoid carriers that can be metabolized anaerobically, particularly alcohols. If possible, use ground water from the site to prepare dosing solutions and to restore water lost from the core barrel during sample collection.

For long-term microcosm studies, autoclaving is the preferred method for sterilization. Nothing available to sterilize core samples works perfectly. Mercuric chloride is excellent for short-term studies (weeks or months). However, mercuric chloride complexes to clays, and control may be lost as it is sorbed over time. Sodium azide is effective in repressing metabolism of bacteria that have cytochromes, but is not effective on strict anaerobes.

The microcosms should be incubated in the dark at the ambient temperature of the aquifer. It is preferable that the microcosms be incubated inverted in an anaerobic glovebox. Anaerobic jars are also available that maintain an oxygen-free environment for the microcosms. Dry redox indicator strips can be placed in the jars to assure that anoxic conditions are maintained. If no anaerobic storage is available, the inverted microcosms can be immersed in approximately two inches of water during incubation. Teflon®-lined butyl rubber septa are excellent for excluding oxygen and should be used if the microcosms must be stored outside an anaerobic environment.

The studies should last from one year to eighteen months. The residence time of a plume may be several years to tens of years at field scale. Rates of transformation that are slow in terms of laboratory experimentation may have a considerable environmental significance. A microcosm study lasting only a few weeks to months may not have the resolution to detect slow changes that are of environmental significance. Additionally, microcosm studies often distinguish a pattern of sequential biodegradation of the contaminants of interest and their daughter products.

C.3.4.7 Microcosm Interpretation

As a practical matter, batch microcosms with an optimal solids/water ratio, that are sampled every two months in triplicate, for up to eighteen months, can resolve biodegradation from abiotic losses with a detection limit of 0.001 to 0.0005 per day. Rates determined from replicated batch microcosms are found to more accurately duplicate field rates of natural attenuation than column studies. Many plumes show significant attenuation of contamination at field calibrated rates that are slower than the detection limit of microcosms. Although rate constants for modeling purposes are more appropriately acquired from field-scale studies, it is reassuring when the rates in the field and the rates in the laboratory agree.

The rates measured in the microcosm study may be faster than the estimated field rate. This may not be due to an error in the laboratory study, particularly if estimation of the field-scale rate of attenuation did not account for regions of preferential flow in the aquifer. The regions of preferential flow may be determined by use of a downhole flow meter or by other methods for determining hydraulic conductivity in one- to two-foot sections of the aquifer.

Statistical comparisons can determine if removals of contaminants of concern in the living treatments are significantly different from zero or significantly different from any sorption that is occurring. Comparisons are made on the first-order rate of removal, that is, the slope of a linear regression of the natural logarithm of the concentration remaining against time of incubation for both the living and control microcosm. These slopes (removal rates) are compared to determine if they are different, and if so, extent of difference that can be detected at a given level of confidence.

C.3.4.8 The Tibbetts Road Case Study

The Tibbetts Road Superfund Site in Barrington, New Hampshire, a former private home, was used to store drums of various chemicals from 1944 to 1984. The primary ground-water contaminants in the overburden and bedrock aquifers were benzene and TCE, with respective concentrations of 7,800 µg/L and 1,100 µg/L. High concentrations of arsenic, chromium, nickel, and lead were also found.

Material collected at the site was used to construct a microcosm study evaluating the removal of benzene, toluene, and TCE. This material was acquired from the most contaminated source at the site, the waste pile near the origin of Segment A (Figure C.3.10). Microcosms were incubated for nine months. The aquifer material was added to 20-mL headspace vials, dosed with 1 mL of spiking solution, capped with a Teflon®-lined, gray butyl rubber septa, and sealed with an aluminum crimp cap. Controls were prepared by autoclaving the material used to construct the microcosms overnight. Initial concentrations for benzene, toluene, and TCE were, respectively, 380 µg/L, 450 µg/L, and 330 µg/L. The microcosms were thoroughly mixed by vortexing, then stored inverted in the dark at the ambient temperature of 10°C.

The results (Figures C.3.11, C.3.12, and C.3.13; Table C.3.9) show that significant biodegradation of both petroleum aromatic hydrocarbons and the chlorinated solvent had occurred. Significant removal in the control microcosms also occurred for all compounds. The data exhibited more variability in the living microcosms than in the control treatment, which is a pattern that has been observed in other microcosm studies. The removals observed in the controls are probably due to sorption; however, this study exhibited more sorption than typically seen.

The rate constants determined from the microcosm study for the three compounds are shown in Table C.3.10. The appropriate rate constant to be used in a model or a risk assessment would be the first-order removal in the living treatment minus the first-order removal in the control, in other words the removal that is in excess of the removal in the controls.

The first-order removal in the living and control microcosms was estimated as the linear regression of the natural logarithm of concentration remaining in each microcosm in each treatment against time of incubation. Student's *t*-distribution with *n*-2 degrees of freedom was used to estimate the 95% confidence interval. The standard error of the difference of the rates of removal in living and control microcosms was estimated as the square root of the sum of the squares of the standard errors of the living and control microcosms, with *n*-4 degrees of freedom (Glantz, 1992).

Table C.3.11 presents the concentrations of organic compounds and their metabolic products in monitoring wells used to define line segments in the aquifer for estimation of field-scale rate constants. Wells in this aquifer showed little accumulation of *trans*-1,2-DCE; 1,1-DCE; vinyl chloride; or ethene, although removals of TCE and *cis*-1,2-DCE were extensive. This can be explained by the observation (Bradley and Chapelle, 1996) that iron-reducing bacteria can rapidly oxidize vinyl chloride to carbon dioxide. Filterable iron accumulated in ground water in this aquifer.

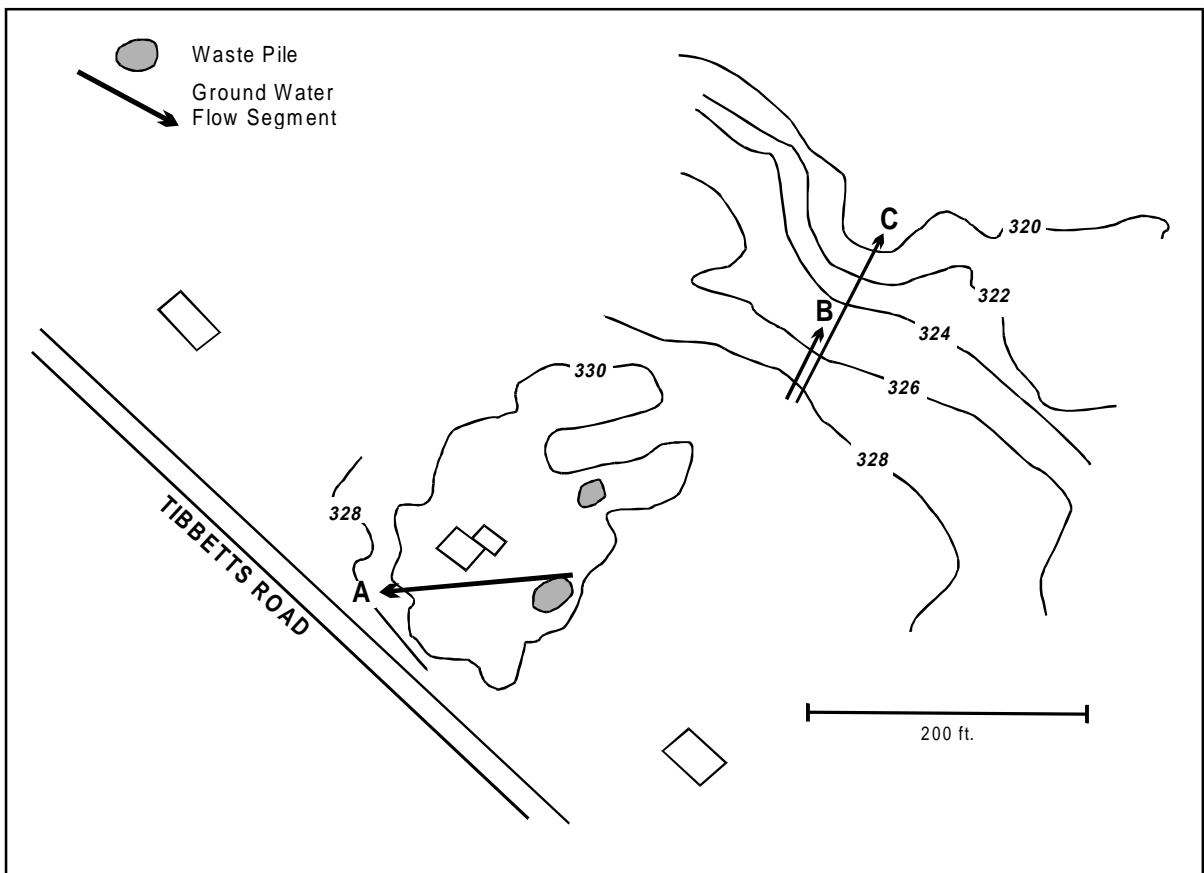


Figure C.3.10 Tibbetts Road study site.

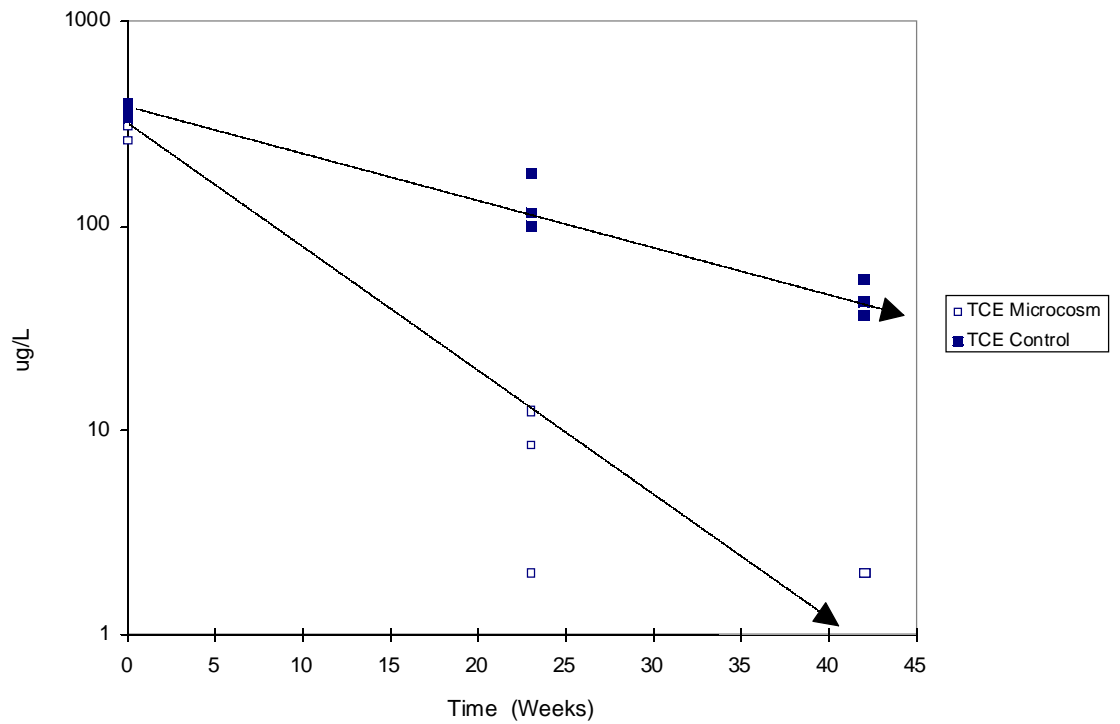


Figure C.3.11 TCE microcosm results.

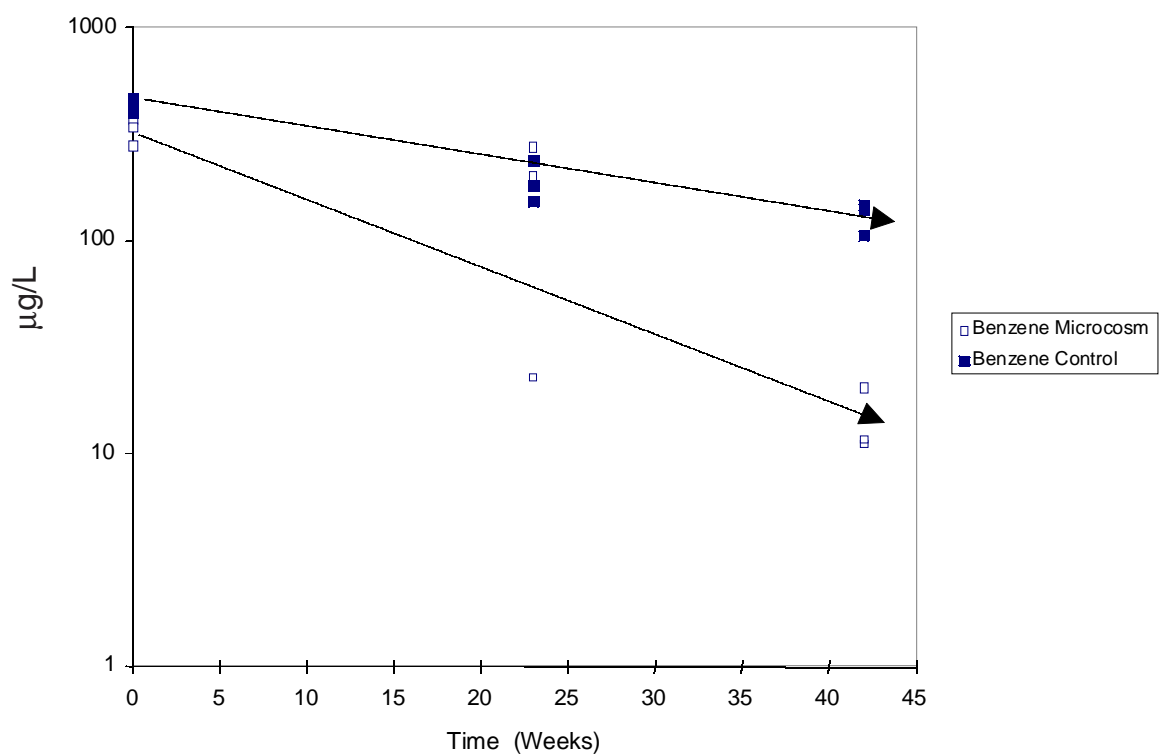


Figure C.3.12 Benzene microcosm results.

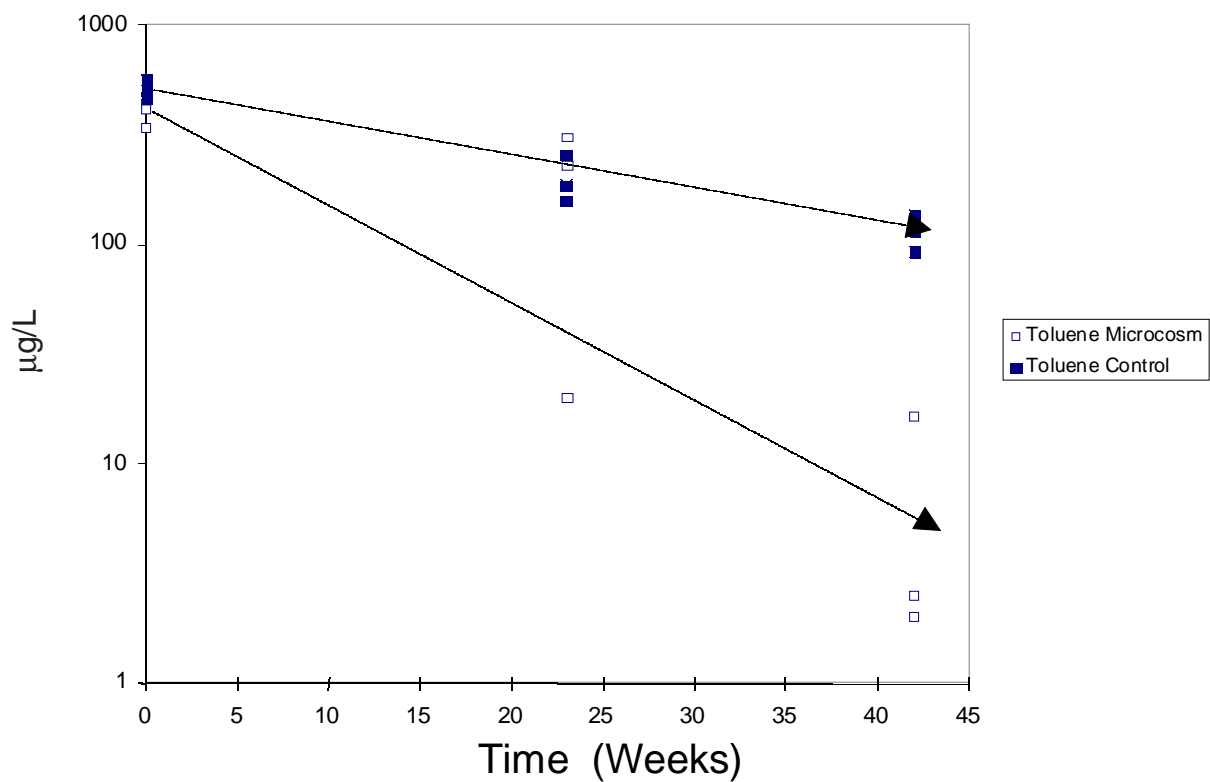


Figure C.3.13 Toluene microcosm results.

Table C.3.9 Concentrations ($\mu\text{g/L}$) of TCE, Benzene, and Toluene in the Tibbetts Road Microcosms

Compound	Time Zero Microcosm	Time Zero Control	Week 23 Microcosm	Week 23 Control	Week 42 Microcosm	Week 42 Control
TCE	328	337	1	180	2	36.3
	261	394	12.5	116	2	54.5
	309	367	8.46	99.9	2	42.3
Mean \pm Standard Deviation	299 \pm 34.5	366 \pm 28.5	7.32 \pm 5.83	132 \pm 42.4	2.0 \pm 0.0	44.4 \pm 9.27
Benzene	366	396	201	236	11.1	146
	280	462	276	180	20.5	105
	340	433	22.8	152	11.6	139
Mean \pm Standard Deviation	329 \pm 44.1	430 \pm 33.1	167 \pm 130	189 \pm 42.8	14.4 \pm 5.29	130 \pm 21.9
Toluene	443	460	228	254	2	136
	342	557	304	185	2.5	92
	411	502	19.9	157	16.6	115
Mean \pm Standard Deviation	399 \pm 51.6	506 \pm 48.6	184 \pm 147	199 \pm 49.9	7.03 \pm 8.29	114 \pm 22.0

The extent of attenuation from well to well listed in Table C.3.11, and the travel time between wells in a segment (Figure C.3.4) were used to calculate first-order rate constants for each segment (Table C.3.12). Travel time between monitoring wells was calculated from site-specific estimates of hydraulic conductivity and from the hydraulic gradient. In the area sampled for the microcosm study, the estimated Darcy flow was 2.0 feet per year. With an estimated porosity in this particular glacial till of 0.1, this corresponds to a plume velocity of 20 feet per year.

C.3.4.9 Summary

Table C.3.13 compares the first-order rate constants estimated from the microcosm studies to the rate constants estimated at field scale. The agreement between the independent estimates of rate is good; indicating that the rates can appropriately be used in a risk assessment. The rates of biodegradation documented in the microcosm study could easily account for the disappearance of trichloroethylene, benzene, and toluene observed at field scale. The rates estimated from the microcosm study are several-fold higher than the rates estimated at field scale. This may reflect an underestimation of the true rate in the field. The estimates of plume velocity assumed that the aquifer was homogeneous. No attempt was made in this study to correct the estimate of plume velocity for the influence of preferential flow paths. Preferential flow paths with a higher hydraulic conductivity than average would result in a faster velocity of the plume, thus a lower residence time and faster rate of removal at field scale.

Table C.3.10 First-order Rate Constants for Removal of TCE, Benzene, and Toluene in the Tibbetts Road Microcosms

Parameter	Living Microcosms	Autoclaved Controls	Removal Above Controls
First-order Rate of Removal (per year)			
TCE	6.31	2.62	3.69
95% Confidence Interval	± 2.50	± 0.50	± 2.31
Minimum Rate Significant at 95% Confidence			1.38
Benzene	3.87	1.51	2.36
95% Confidence Interval	± 1.96	± 0.44	± 1.83
Minimum Rate Significant at 95% Confidence			0.53
Toluene	5.49	1.86	3.63
95% Confidence Interval	± 2.87	± 0.45	± 2.64
Minimum Rate Significant at 95% Confidence			0.99

Table C.3.11 Concentrations of Contaminants and Metabolic By-products in Monitoring Wells along Segments in the Plume used to Estimate Field-scale Rate Constants

Parameter	Segment A		Segment B		Segment C	
Monitoring Well	80S	79S	70S	52S	70S	53S
	Upgradient	Downgradient	Up gradient	Down gradient	Upgradient	Down gradient
	-----($\mu\text{g/liter}$)-----					
TCE	200	13.7	710	67	710	3.1
<i>cis</i> -1,2-DCE	740	10.9	220	270	220	2.9
<i>trans</i> -1,2-DCE	0.41	<1	0.8	0.3	0.8	<1
1,1-DCE	0.99	<1	<1	1.6	<1	<1
Vinyl Chloride	<1	<1	<1	<1	<1	<1
Ethene	<4	<4	7	<4	7	<4
Benzene	510	2.5	493	420	493	<1
Toluene	10000	<1	3850	900	3850	<1
<i>o</i> -Xylene	1400	8.4	240	71	240	<1
<i>m</i> -Xylene	2500	<1	360	59	360	<1
<i>p</i> -Xylene	1400	22	1100	320	1100	<1
Ethylbenzene	1300	0.7	760	310	760	<1
Methane	353	77	8	3	8	<2
Iron						27000

Table C.3.12 First-order Rate Constants for Contaminant Attenuation in Segments of the Tibbetts Road Plume

Flow Path Segments in Length and Time of Ground-water Travel			
	Segment A 130 feet = 6.5 years	Segment B 80 feet = 4.0 years	Segment C 200 feet = 10 years
Compound	First-order Rate Constants in Segments (per year)		
TCE	0.41	0.59	0.54
cis-1,2-DCE	0.65	produced	0.43
Benzene	0.82	0.04	>0.62
Toluene	>1.42	0.36	>0.83
o-Xylene	0.79	0.30	>0.55
m-Xylene	>1.20	0.45	>0.59
p-Xylene	0.64	0.31	>0.70
Ethylbenzene	1.16	0.22	>0.66

Table C.3.13 Comparison of First-order Rate Constants in a Microcosm Study, and in the Field, at the Tibbetts Road NPL Site

Parameter	Microcosms Corrected for Controls		Field Scale		
	Average Rate	Minimum Rate Significant at 95% Confidence	Segment A	Segment B	Segment C
	-----First-order Rate (per year)-----				
Trichloroethylene	3.69	1.38	0.41	0.59	0.54
Benzene	2.36	0.53	0.82	0.04	>0.62
Toluene	3.63	0.99	>1.42	0.36	>0.83